



doi: 10.3969/j. issn. 1673-9736. 2025. 02. 01

Article ID: 1673-9736 (2025) 02-0079-20

# Detrital zircon U–Pb ages of sandstone from Jiufengshan Formation in Nenjiang area, Heilongjiang Province: Provenance and tectonic implications

JIA Xianghe<sup>1</sup>, LIANG Chenyue<sup>1,2\*</sup> and ZHENG Changqing<sup>1,2</sup>

1. College of Earth Sciences, Jilin University, Changchun 130061, China;

2. Key Laboratory of Mineral Resources Evaluation in Northeast Asia, Ministry of Natural Resources, Jilin University, Changchun 130026, China

**Abstract:** During Early Cretaceous, NNE-trending extensional basins filling with various volcanic-sedimentary formations developed in the northeastern Da Hinggan Ling (Mts.), northeastern China. This study investigates the formation age and geological background of Jiufengshan Formation, providing insights into its tectonic setting and formation mechanisms. Detrital zircons from four sandstone samples of Jiufengshan Formation in Nenjiang area indicate a maximum depositional age of  $116 \pm 1$  Ma, corresponding to late Early Cretaceous. Petrographic analysis and zircon age peak comparisons suggest these sandstones originated from proximal deposits with nearby provenances of earlier and contemporaneous volcanic rocks. Further research on the sandstone framework and trace elements in detrital zircons indicates that the formation process of Jiufengshan Formation was likely related to the low-angle subduction of the Paleo-Pacific plate.

**Keywords:** Jiufengshan Formation; Da Hinggan Ling (Mts.); Early Cretaceous; detrital zircon

## Introduction

The Central Asian Orogenic Belt (CAOB) is one of the largest and longest-evolving accretionary orogenic belts on Earth (Sengör *et al.*, 1993, 2018; Xiao *et al.*, 2009), which is situated among the Siberian, East European, Tarim and North China cratons, extending from the Ural Mountains to the Pacific coast (Jahn *et al.*, 2000; Xiao *et al.*, 2003, 2015; Wilde, 2015). The northeastern China, part of the eastern segment of the CAOB, is referred to the Xing'an–Mongolian Orogenic Belt (XMOB) (Liu *et al.*, 2017b, 2021; Zhang *et al.*, 2019; Guan *et al.*, 2019), which witnessed the closure of the Paleo-

Asian Ocean and the amalgamation of multiple microcontinental massifs or terranes (Wu *et al.*, 2011; Tang *et al.*, 2013; Zhou *et al.*, 2013; Zhou *et al.*, 2015; Wilde, 2015; Fu *et al.*, 2016, 2018; Mi *et al.*, 2017; Guan *et al.*, 2019; Li *et al.*, 2019) (Fig.1). During early Mesozoic, the tectonic evolution of northeastern China was dominated by the closure of the eastern Paleo-Asian Ocean. Subsequently, in late Mesozoic, widespread NW–SE extensional structures developed, which influenced by superposition and transformation from both the Mongol–Okhotsk tectonic domain in the northwest and the Paleo-Pacific tectonic domain in the east (Wu *et al.*, 2007; Zhou *et al.*, 2009; Li *et al.*, 2017) (Fig.1). During Early Cretaceous, a series

Received 16 December 2024, accepted 15 January 2025

Supported by the National Key R&D Program (No. 2017YFC0601401-03).

\*Corresponding author (E-mail: chenyueliang@jlu.edu.cn)

of NNE-trending faulted basins characterized by the development of the volcanic-sedimentary formations, e.g., Ganhe Formation, Jiufengshan Formation and Guanghua Formation, were formed in northeastern Da Hinggan Ling (Mts.). The dynamic mechanisms of these formations remain unclear (Liu *et al.*, 2008b; Yang *et al.*, 2020).

Detrital zircons are resilient to weathering, erosion, abrasion, and thermal alteration, enabling their survival through multiple transportation events while retaining a stable U–Pb isotopic system (Bruguier & Lancelet, 1997; Lee *et al.*, 1997; Cherniak & Watson, 2000). Research shows that zircons in clastic sediments reflect provenance characteristics and illustrate the relationship between basin subsidence and tectonic thermal events (Carter & Steve, 1999; Fedo *et al.*, 2003; Griffin *et al.*, 2004; Moecher & Samson, 2006; Kelty *et al.*, 2008). This paper aims to integrate petrology, zircon U–Pb geochronology and trace element geochemistry of detrital zircons to determine the provenance and tectonic setting of

sandstones from Jiufengshan Formation in Nenjiang area of northeastern Da Hinggan Ling (Mts.).

## 1 Geological setting

The Da Hinggan Ling (Mts.) in northeastern China (Fig.1) provides a comprehensive record of Mesozoic evolution (Jiang *et al.*, 2010; Wu *et al.*, 2011; Xu *et al.*, 2013; Ouyang *et al.*, 2015; Yuan *et al.*, 2018). During Early Cretaceous, the Dayangshu and Heibaoshan–Handaqi basins formed in northeastern Da Hinggan Ling (Mts.), characterized by the deposition of the Jiufengshan Formation in Nenjiang area (Liu *et al.*, 2008b; Yang *et al.*, 2020). Defined by the 109<sup>th</sup> team of the Heilongjiang Coalfield Geological Exploration Bureau in 1973 in the Dayangshu Basin, the Jiufengshan Formation consists of sedimentary, volcanic and volcaniclastic rocks, along with plant fossils (Liu *et al.*, 2008b; Tong *et al.*, 2008) (Fig.2). It is located on the northeastern slope of the Da Hinggan Ling (Mts.) and the northwestern slope of the Xiao Hinggan Ling (Mts.), in conformable contact with

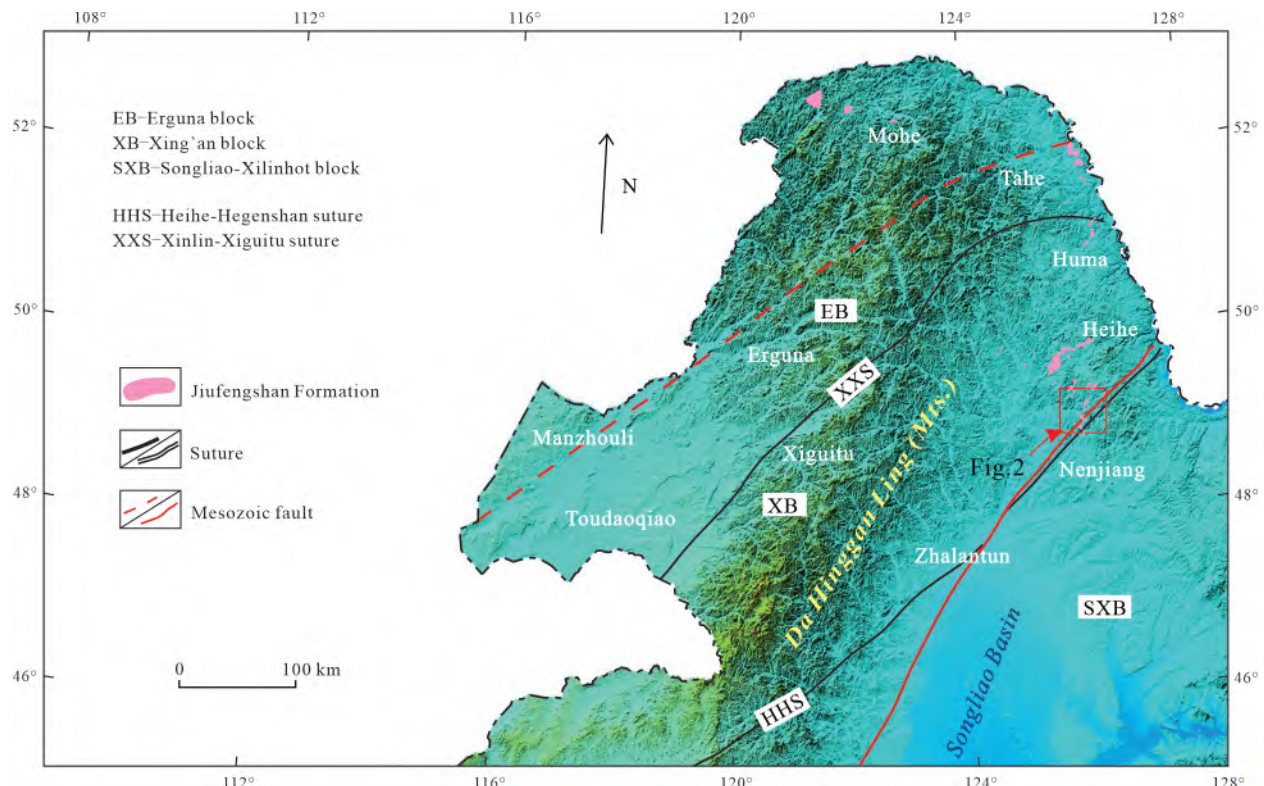


**Fig.1** Main tectonic features in northeastern China (modified after Liu *et al.*, 2017b; Liang *et al.*, 2019)

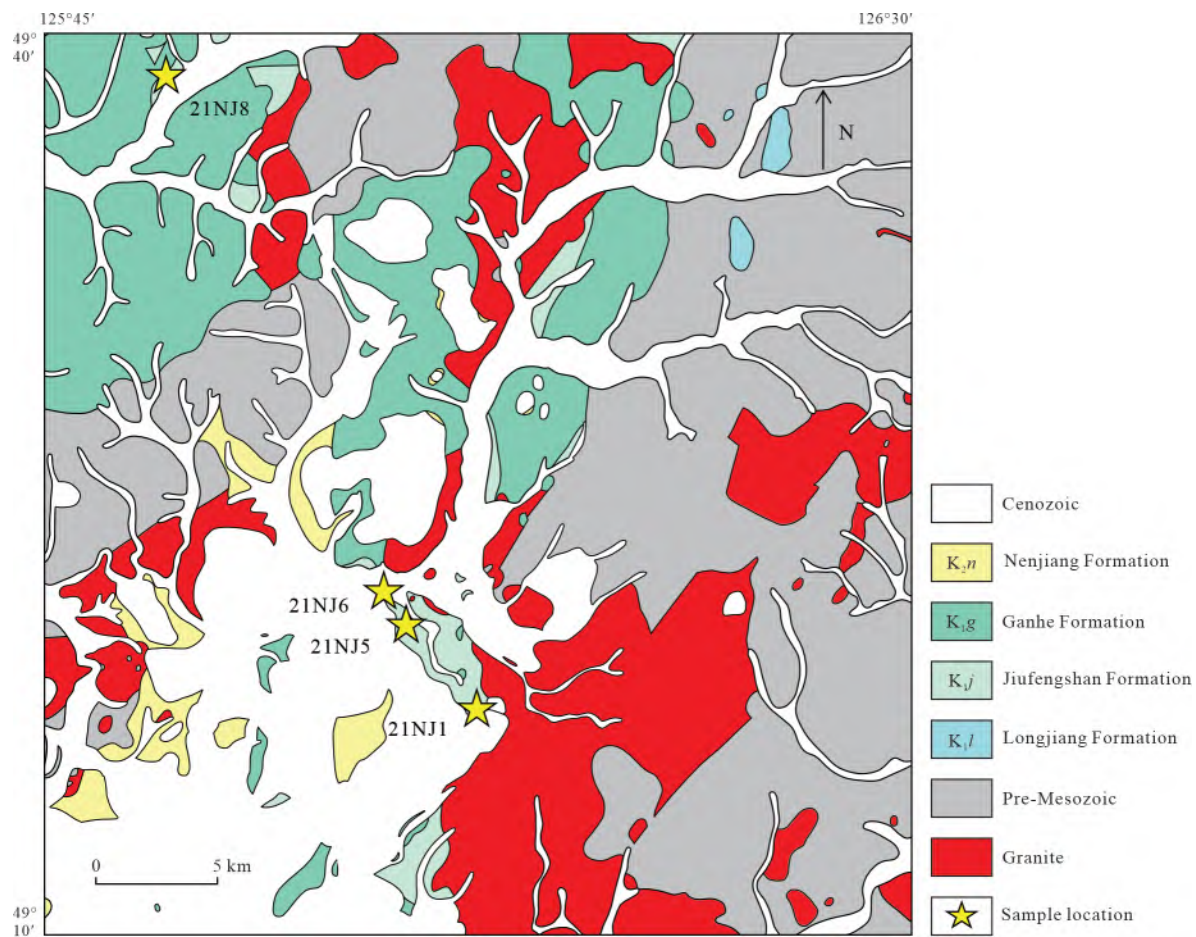


**Fig.2** Detailed geological map with sampling locations (modified after Song *et al.*, 2022)

the overlying Ganhe Formation and the underlying Guanghua Formation. This paper presents an analysis of four sandstone samples from the Jiufengshan Formation through framework analysis and detrital zircon dating.

## 2 Sample descriptions

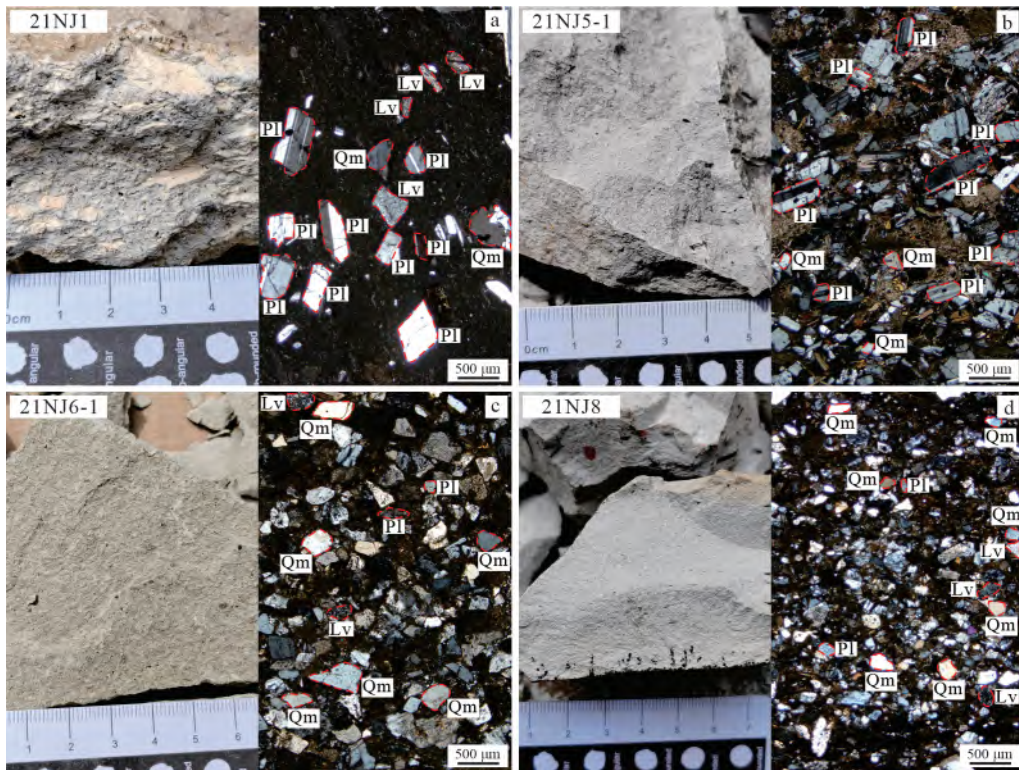
Microscopic examination of sandstone samples (21NJ1, 21NJ5-1, 21NJ6-1 and 21NJ8) from the Jiufengshan Formation reveals similar immature textures (Fig.3a-d; Table 1). These samples are poorly sorted and primarily consist of angular clastics, indicating low textural and compositional maturity. The detrital grains mainly include lithic fragments, feldspar and quartz. The lithic fragments are predominantly andesitic, with a minor presence of rhyolitic fragments. Feldspar is mainly plagioclase with minor

potassium feldspar, while quartz is predominantly monocrystalline, exhibiting surface cracks and slight undulating extinction with sub-grains.

## 3 Analytical methods

### 3.1 Sandstone framework analysis

The method for reconstructing provenance based on framework constituent analysis was originated from Dickinson *et al.* (1983), who summarized sandstone detrital compositions across various global areas and tectonic settings, and established discrimination diagrams to differentiate provenance based on sandstone compositions and modal contents. Garzanti (2019) later refined this method. It involves statistical data on constituents observed under the microscope, representing tectonic settings through triangular



Abbreviations: Lv, lithic volcanic fragment; Pl, plagioclase; Qm, monocrystalline quartz.

**Fig.3 Typical macro- and micro-photographs**

diagrams such as Qt–F–L and Qm–F–Lt diagrams. In these diagrams, Qt denotes total quartz (Qm for monocrystalline quartz and Qp for polycrystalline quartz), F represents feldspar (Kf for K-feldspar and Pl for plagioclase), and Lt refers to total lithic (Lv for lithic volcanic fragment, Ls for lithic sedimentary fragment and Qp). In our study, we counted over 300 grains per thin section, recording the number and size of different components to prepare for tectonic discrimination diagrams from Dickinson *et al.* (1983). Data are presented in Table 1.

**Table 1 Detrital component contents (%) of sandstones from Jiufengshan Formation**

Sample No.	Qt	F	L	Qm	F	Lt
21NJ1	20	44	36	19	44	37
21NJ5-1	23	38	39	22	38	40
21NJ6-1	24	36	40	23	36	41
21NJ8	19	41	40	18	41	41

### 3.2 Zircon U–Pb dating

The LA–ICP–MS zircon U–Pb dating of four

sandstone samples was performed at the Key Laboratory of Mineral Resources Evaluation in Northeast Asia, Ministry of Natural Resources, Jilin University. To ensure representative ages, at least 60 zircon grains were selected from each sandstone sample. Helium gas was employed as the carrier gas to minimize aerosol deposition at the ablation site and in transport tubing (Andersen, 2002; Jackson *et al.*, 2004; Vermeesch, 2004). The analysis utilized a 7500A mass spectrometer with a German 193-ArF excimer laser, featuring a 32 μm ablation spot diameter and a frequency of 7 Hz. The U–Pb isotope fractionation corrections were based on the external age standards of 91500 and GJ-1, while the NIST610 glass standard was employed for the Pb, U and Th content calculations. Age distribution diagrams were generated using  $^{206}\text{Pb}/^{238}\text{U}$  for grains younger than 1 Ga and  $^{207}\text{Pb}/^{206}\text{Pb}$  for those older than 1 Ga. All dated zircon grains have a concordance within  $\pm 10\%$ .

## 4 Results

### 4.1 Sandstone framework analysis

The mineral content of four typical sandstone samples from the Jiufengshan Formation was analyzed, and the results are presented in Table 1. In the provenance discrimination diagram, all samples fall within the transitional arc region (Fig.4).

### 4.2 Zircon U-Pb dating

The selected zircons from four dated sandstone samples are euhedral to subhedral, with sizes ranging from 60 to 120  $\mu\text{m}$  (Fig.5), showing clear internal structures and typical oscillatory growth zoning in CL images. Their Th/U ratios (0.05–3.57) indicate a magmatic origin (Pupin, 1980; Koschek, 1993; Hoskin

& Schaltegger, 2003) (Table 2).

For sample 21NJ1, 120 zircons were analyzed, yielding 114 with less than 10% discordance (Table 2). The  $^{206}\text{Pb}/^{238}\text{U}$  ages from these grains ranged from  $875\pm20$  Ma to  $113\pm5$  Ma (Fig.6a), and divided into seven groups: 875 Ma, 633 Ma, 469 Ma, 374–283 Ma (66 grains, peak at 306 Ma), 253–202 Ma (37 grains, peak at 225 Ma), 185–161 Ma (6 grains, peak at 172 Ma), and 120–113 Ma (2 grains).

In sample 21NJ5-1, 70 zircons were analyzed, with 67 yielding less than 10% discordance (Table 2). The  $^{206}\text{Pb}/^{238}\text{U}$  ages from these concordant zircon grains ranged from  $524\pm14$  Ma to  $118\pm6$  Ma (Fig.6b), organized into four groups: 524 Ma, 342–277 Ma (59 grains, peak at 303 Ma), 248–221 Ma (5 grains, peak at 236 Ma), and 125–118 Ma (2 grains).

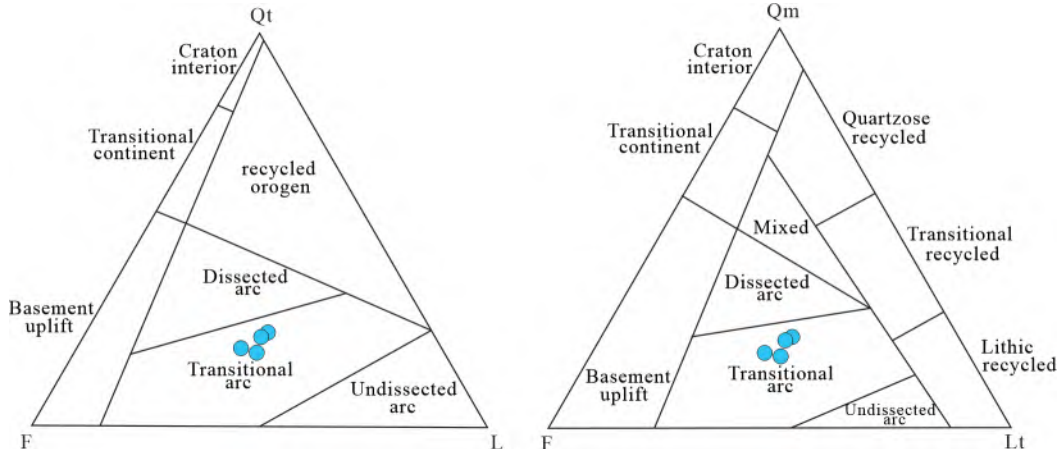


**Fig.4** Provenance discrimination diagram of sandstone from Jiufengshan Formation (modified after Dickinson *et al.*, 1983)

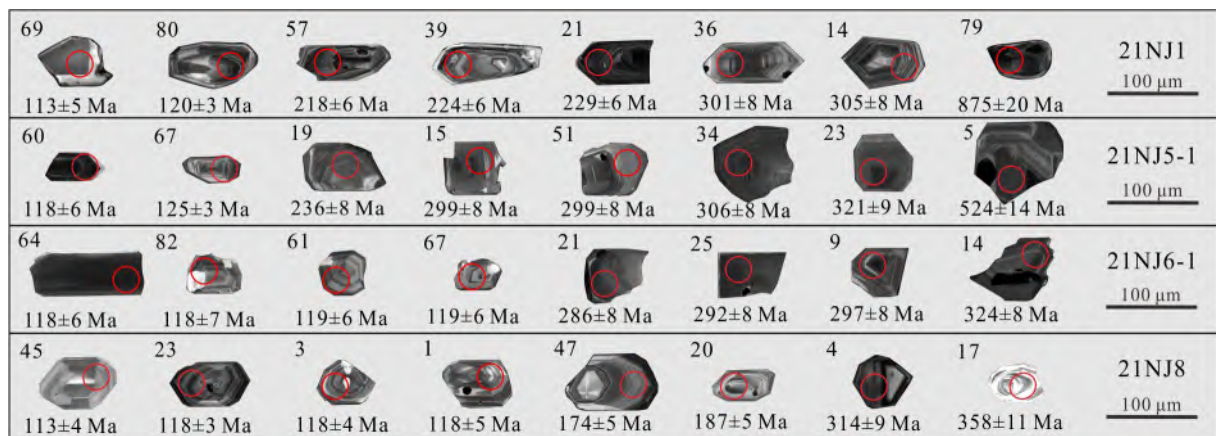


**Fig.5** Cathodoluminescence images of representative zircons of sandstones from Jiufengshan Formation

**Table 2** Zircon U-Pb dating results of detrital zircons from Jiufengshan Formation

No.	Isotopic ratio						Age/Ma						Th/U
	$^{207}\text{Pb}/^{206}\text{Pb}$	1 $\sigma$	$^{207}\text{Pb}/^{235}\text{U}$	1 $\sigma$	$^{206}\text{Pb}/^{238}\text{U}$	1 $\sigma$	$^{207}\text{Pb}/^{206}\text{Pb}$	1 $\sigma$	$^{207}\text{Pb}/^{235}\text{U}$	1 $\sigma$	$^{206}\text{Pb}/^{238}\text{U}$	1 $\sigma$	
21NJ1-1	0.051 1	0.001 4	0.242 4	0.007 5	0.034 4	0.000 9	246	32	220	6	218	5	0.40
21NJ1-2	0.056 6	0.004 2	0.419 4	0.030 5	0.053 8	0.001 7	476	104	356	22	338	11	0.63
21NJ1-3	0.052 4	0.002 0	0.271 2	0.010 9	0.037 5	0.001 0	303	47	244	9	238	6	0.37
21NJ1-4	0.049 3	0.002 2	0.271 7	0.012 6	0.040 0	0.001 1	160	60	244	10	253	7	0.39
21NJ1-5	0.052 3	0.001 5	0.358 8	0.011 4	0.049 8	0.001 3	299	33	311	9	313	8	0.33
21NJ1-6	0.050 8	0.001 7	0.250 2	0.009 1	0.035 8	0.000 9	229	41	227	7	226	6	0.71
21NJ1-7	0.050 7	0.001 6	0.258 1	0.008 9	0.036 9	0.001 0	229	38	233	7	234	6	0.36
21NJ1-8	0.054 0	0.006 0	0.368 9	0.039 6	0.049 6	0.001 9	371	171	319	29	312	12	0.55
21NJ1-9	0.051 2	0.001 7	0.269 1	0.009 6	0.038 1	0.001 0	250	39	242	8	241	6	0.31
21NJ1-10	0.052 7	0.005 2	0.377 2	0.036 1	0.051 9	0.001 9	316	151	325	27	326	12	0.66
21NJ1-11	0.053 5	0.004 2	0.372 1	0.028 3	0.050 4	0.001 6	352	114	321	21	317	10	0.60
21NJ1-12	0.052 8	0.004 8	0.375 5	0.033 7	0.051 6	0.001 8	321	141	324	25	324	11	0.62
21NJ1-13	0.054 2	0.004 1	0.420 2	0.031 4	0.056 3	0.001 8	378	110	356	22	353	11	0.60
21NJ1-14	0.052 7	0.002 2	0.352 2	0.015 2	0.048 5	0.001 3	315	52	306	11	305	8	0.45
21NJ1-15	0.053 3	0.003 5	0.400 9	0.026 0	0.054 6	0.001 7	342	92	342	19	342	10	0.62
21NJ1-16	0.050 0	0.002 1	0.241 5	0.010 4	0.035 1	0.000 9	194	53	220	9	222	6	0.72
21NJ1-17	0.053 5	0.003 8	0.414 9	0.029 2	0.056 3	0.001 8	349	103	352	21	353	11	0.47
21NJ1-18	0.050 1	0.004 9	0.194 6	0.018 7	0.028 2	0.001 0	201	150	181	16	179	6	0.75
21NJ1-19	0.052 4	0.005 6	0.353 7	0.036 7	0.049 0	0.001 9	302	165	308	28	308	11	0.51
21NJ1-20	0.049 7	0.003 6	0.173 0	0.012 2	0.025 3	0.000 8	179	104	162	11	161	5	0.60
21NJ1-21	0.051 1	0.001 5	0.254 7	0.008 2	0.036 1	0.000 9	247	34	230	7	229	6	0.33
21NJ1-22	0.053 1	0.004 9	0.356 3	0.031 9	0.048 7	0.001 7	333	140	309	24	306	10	0.48
21NJ1-23	0.053 4	0.006 2	0.391 0	0.043 9	0.053 1	0.002 2	345	179	335	32	334	13	0.75
21NJ1-24	0.052 9	0.003 8	0.344 3	0.024 5	0.047 2	0.001 5	324	105	300	19	297	9	0.55
21NJ1-25	0.052 9	0.004 5	0.367 3	0.030 3	0.050 3	0.001 7	326	126	318	22	316	10	0.58
21NJ1-26	0.053 5	0.002 0	0.364 2	0.014 1	0.049 4	0.001 3	350	44	315	10	311	8	0.56
21NJ1-27	0.053 9	0.004 8	0.420 9	0.036 5	0.056 7	0.002 0	366	134	357	26	355	12	1.02
21NJ1-28	0.051 0	0.004 5	0.257 1	0.022 4	0.036 6	0.001 3	239	134	232	18	232	8	0.79
21NJ1-29	0.056 2	0.003 0	0.585 3	0.031 0	0.075 5	0.002 2	461	68	468	20	469	13	0.53
21NJ1-30	0.053 0	0.002 3	0.344 4	0.015 1	0.047 1	0.001 3	328	53	300	11	297	8	1.28
21NJ1-31	0.053 5	0.001 9	0.401 1	0.014 9	0.054 4	0.001 4	348	41	342	11	342	9	0.70
21NJ1-32	0.053 4	0.004 1	0.393 3	0.029 8	0.053 5	0.001 7	345	113	337	22	336	11	0.54
21NJ1-33	0.055 6	0.004 6	0.264 3	0.021 4	0.034 5	0.001 2	436	121	238	17	219	7	0.58
21NJ1-34	0.050 4	0.001 8	0.246 5	0.009 0	0.035 5	0.000 9	213	41	224	7	225	6	0.40
21NJ1-35	0.054 2	0.003 1	0.416 6	0.023 7	0.055 8	0.001 6	378	77	354	17	350	10	0.77
21NJ1-36	0.052 1	0.002 1	0.342 9	0.014 2	0.047 8	0.001 3	289	49	299	11	301	8	1.16
21NJ1-37	0.052 7	0.003 0	0.341 0	0.019 5	0.047 0	0.001 4	315	78	298	15	296	8	1.04
21NJ1-38	0.054 0	0.003 6	0.404 0	0.026 4	0.054 2	0.001 7	372	93	345	19	340	10	0.80
21NJ1-39	0.051 2	0.002 4	0.250 1	0.011 8	0.035 4	0.001 0	251	60	227	10	224	6	0.38
21NJ1-40	0.052 0	0.005 1	0.350 7	0.033 7	0.048 9	0.001 8	286	151	305	25	308	11	0.56
21NJ1-41	0.050 6	0.003 3	0.244 8	0.015 8	0.035 1	0.001 1	220	94	222	13	223	7	0.65
21NJ1-42	0.053 6	0.004 6	0.407 8	0.034 3	0.055 2	0.001 9	353	128	347	25	346	12	0.91
21NJ1-43	0.053 0	0.005 0	0.358 2	0.033 2	0.049 0	0.001 8	330	145	311	25	308	11	0.54
21NJ1-44	0.049 4	0.002 7	0.335 5	0.018 1	0.049 3	0.001 4	164	75	294	14	310	8	0.85
21NJ1-45	0.052 7	0.001 9	0.271 3	0.010 1	0.037 4	0.001 0	314	42	244	8	237	6	0.99
21NJ1-46	0.052 0	0.003 5	0.343 9	0.023 1	0.048 0	0.001 5	285	99	300	17	302	9	0.51
21NJ1-47	0.053 3	0.003 7	0.367 5	0.025 2	0.050 0	0.001 5	342	100	318	19	315	9	0.53
21NJ1-48	0.052 2	0.002 6	0.336 0	0.016 5	0.046 7	0.001 3	295	64	294	13	294	8	0.79
21NJ1-49	0.052 5	0.004 9	0.364 3	0.032 9	0.050 3	0.001 8	307	141	315	24	316	11	0.61

(continued Table 2)

No.	Isotopic ratio						Age/Ma						Th/U
	$^{207}\text{Pb}/^{206}\text{Pb}$	1 $\sigma$	$^{207}\text{Pb}/^{235}\text{U}$	1 $\sigma$	$^{206}\text{Pb}/^{238}\text{U}$	1 $\sigma$	$^{207}\text{Pb}/^{206}\text{Pb}$	1 $\sigma$	$^{207}\text{Pb}/^{235}\text{U}$	1 $\sigma$	$^{206}\text{Pb}/^{238}\text{U}$	1 $\sigma$	
21NJ1-50	0.053 8	0.002 8	0.426 8	0.022 3	0.057 6	0.001 6	362	68	361	16	361	10	0.55
21NJ1-51	0.052 3	0.004 9	0.353 6	0.032 2	0.049 1	0.001 7	297	142	307	24	309	11	0.58
21NJ1-52	0.050 6	0.002 5	0.242 2	0.012 1	0.034 7	0.001 0	224	66	220	10	220	6	0.70
21NJ1-53	0.052 0	0.002 8	0.345 1	0.018 4	0.048 1	0.001 4	285	72	301	14	303	8	0.65
21NJ1-54	0.058 0	0.003 7	0.427 3	0.026 8	0.053 5	0.001 6	529	85	361	19	336	10	0.70
21NJ1-55	0.052 6	0.004 8	0.343 9	0.030 7	0.047 4	0.001 6	310	140	300	23	299	10	0.56
21NJ1-56	0.051 5	0.003 9	0.333 6	0.024 6	0.047 0	0.001 5	264	111	292	19	296	9	0.68
21NJ1-57	0.050 0	0.001 8	0.237 2	0.009 0	0.034 4	0.000 9	195	44	216	7	218	6	0.86
21NJ1-58	0.049 9	0.002 5	0.228 0	0.011 4	0.033 2	0.000 9	188	66	209	9	210	6	0.45
21NJ1-59	0.051 6	0.003 4	0.326 1	0.021 5	0.045 8	0.001 4	269	97	287	16	289	8	0.62
21NJ1-60	0.047 5	0.003 9	0.316 4	0.025 4	0.048 4	0.001 5	74	120	279	20	304	9	0.49
21NJ1-61	0.051 2	0.001 8	0.421 7	0.015 3	0.059 8	0.001 5	252	42	357	11	374	9	0.60
21NJ1-62	0.050 5	0.003 7	0.341 1	0.024 4	0.049 0	0.001 5	218	110	298	18	309	9	0.69
21NJ1-63	0.055 1	0.004 1	0.390 0	0.028 1	0.051 4	0.001 6	414	106	334	21	323	10	0.49
21NJ1-64	0.049 7	0.004 2	0.308 1	0.025 4	0.045 1	0.001 5	179	126	273	20	284	9	0.30
21NJ1-65	0.046 9	0.004 7	0.244 4	0.024 0	0.037 9	0.001 3	42	151	222	20	240	8	0.55
21NJ1-66	0.048 4	0.003 1	0.318 5	0.020 3	0.047 8	0.001 4	121	91	281	16	301	8	1.05
21NJ1-67	0.047 2	0.002 1	0.229 8	0.010 2	0.035 4	0.000 9	58	54	210	8	224	6	0.96
21NJ1-68	0.051 3	0.003 5	0.416 7	0.028 2	0.059 0	0.001 7	256	101	354	20	369	11	0.60
21NJ1-69	0.046 9	0.011 4	0.114 5	0.027 3	0.017 7	0.000 8	45	404	110	25	113	5	0.96
21NJ1-70	0.045 4	0.003 6	0.172 0	0.013 5	0.027 5	0.000 8	—	113	161	12	175	5	0.63
21NJ1-71	0.063 7	0.001 7	0.905 1	0.025 9	0.103 2	0.002 5	731	27	654	14	633	15	0.34
21NJ1-72	0.051 6	0.001 5	0.250 9	0.007 9	0.035 3	0.000 9	268	34	227	6	224	5	0.66
21NJ1-73	0.049 1	0.001 4	0.248 9	0.007 6	0.036 8	0.000 9	154	33	226	6	233	6	0.39
21NJ1-74	0.052 7	0.001 9	0.420 0	0.015 9	0.057 9	0.001 5	315	43	356	11	363	9	0.68
21NJ1-75	0.050 2	0.002 0	0.240 3	0.009 7	0.034 8	0.000 9	206	49	219	8	220	6	1.10
21NJ1-76	0.058 2	0.003 2	0.476 9	0.026 1	0.059 5	0.001 7	539	71	396	18	372	10	1.32
21NJ1-77	0.058 5	0.003 4	0.395 8	0.022 9	0.049 1	0.001 4	550	76	339	17	309	9	0.75
21NJ1-78	0.057 0	0.005 5	0.383 3	0.036 1	0.048 8	0.001 8	492	143	329	26	307	11	0.63
21NJ1-79	0.067 7	0.001 7	1.354 9	0.037 0	0.145 3	0.003 5	860	25	870	16	875	20	0.56
21NJ1-80	0.048 1	0.002 7	0.124 6	0.006 9	0.018 8	0.000 5	105	75	119	6	120	3	0.55
21NJ1-81	0.054 0	0.001 5	0.269 8	0.008 1	0.036 3	0.000 9	369	31	243	6	230	6	0.54
21NJ1-82	0.049 5	0.001 5	0.234 6	0.007 7	0.034 4	0.000 9	173	36	214	6	218	5	0.64
21NJ1-83	0.053 6	0.002 4	0.373 1	0.016 8	0.050 5	0.001 3	356	55	322	12	318	8	0.36
21NJ1-84	0.054 3	0.001 4	0.265 5	0.007 7	0.035 5	0.000 9	384	29	239	6	225	5	0.43
21NJ1-85	0.057 3	0.003 5	0.353 9	0.021 1	0.044 9	0.001 3	502	81	308	16	283	8	0.61
21NJ1-86	0.051 7	0.002 1	0.381 9	0.016 1	0.053 7	0.001 4	273	51	328	12	337	9	0.52
21NJ1-87	0.050 4	0.001 9	0.331 4	0.013 2	0.047 8	0.001 2	213	47	291	10	301	8	0.94
21NJ1-88	0.051 0	0.001 9	0.349 6	0.013 4	0.049 8	0.001 3	242	45	304	10	313	8	1.16
21NJ1-89	0.054 4	0.004 5	0.218 1	0.017 5	0.029 1	0.001 0	387	122	200	15	185	6	0.51
21NJ1-90	0.049 9	0.002 9	0.224 6	0.011 7	0.032 6	0.000 8	191	133	206	10	207	5	0.35
21NJ1-91	0.057 4	0.002 8	0.422 9	0.020 6	0.053 5	0.001 5	506	60	358	15	336	9	0.54
21NJ1-92	0.056 6	0.002 5	0.415 9	0.019 0	0.053 3	0.001 4	478	55	353	14	335	9	0.56
21NJ1-93	0.053 9	0.002 3	0.265 4	0.011 8	0.035 8	0.001 0	365	54	239	9	227	6	0.84
21NJ1-94	0.050 3	0.002 3	0.255 6	0.011 8	0.036 9	0.001 0	210	59	231	10	233	6	0.55
21NJ1-95	0.051 6	0.001 9	0.343 6	0.013 2	0.048 4	0.001 3	266	44	300	10	305	8	0.74
21NJ1-96	0.049 5	0.001 3	0.181 9	0.005 4	0.026 7	0.000 7	173	31	170	5	170	4	0.57
21NJ1-97	0.055 4	0.002 1	0.259 1	0.010 3	0.033 9	0.000 9	429	45	234	8	215	6	1.16
21NJ1-98	0.050 5	0.001 4	0.248 9	0.007 5	0.035 8	0.000 9	217	32	226	6	227	6	0.36

(continued Table 2)

No.	Isotopic ratio						Age/Ma						Th/U
	$^{207}\text{Pb}/^{206}\text{Pb}$	1 $\sigma$	$^{207}\text{Pb}/^{235}\text{U}$	1 $\sigma$	$^{206}\text{Pb}/^{238}\text{U}$	1 $\sigma$	$^{207}\text{Pb}/^{206}\text{Pb}$	1 $\sigma$	$^{207}\text{Pb}/^{235}\text{U}$	1 $\sigma$	$^{206}\text{Pb}/^{238}\text{U}$	1 $\sigma$	
21NJ1-99	0.055 8	0.003 1	0.362 8	0.020 0	0.047 2	0.001 3	446	73	314	15	297	8	0.79
21NJ1-100	0.051 7	0.004 3	0.369 2	0.028 9	0.051 8	0.001 4	272	190	319	21	326	9	0.53
21NJ1-101	0.053 3	0.001 4	0.259 8	0.007 5	0.035 3	0.000 9	343	29	235	6	224	5	0.33
21NJ1-102	0.051 0	0.006 6	0.336 7	0.041 9	0.047 9	0.001 6	241	281	295	32	302	10	0.61
21NJ1-103	0.054 5	0.002 5	0.239 6	0.011 3	0.031 9	0.000 9	391	59	218	9	202	5	0.88
21NJ1-104	0.050 6	0.002 0	0.236 9	0.009 6	0.033 9	0.000 9	224	49	216	8	215	6	0.46
21NJ1-105	0.055 6	0.002 8	0.389 6	0.019 6	0.050 8	0.001 4	436	64	334	14	320	9	0.64
21NJ1-106	0.055 8	0.002 1	0.274 6	0.010 6	0.035 7	0.000 9	444	43	246	8	226	6	0.66
21NJ1-107	0.052 1	0.001 5	0.242 9	0.007 6	0.033 8	0.000 9	292	33	221	6	214	5	0.28
21NJ1-108	0.052 4	0.003 7	0.343 8	0.024 0	0.047 5	0.001 5	304	103	300	18	299	9	0.54
21NJ1-109	0.058 2	0.002 3	0.427 3	0.017 4	0.053 2	0.001 4	539	45	361	12	334	9	0.74
21NJ1-110	0.053 7	0.002 8	0.410 2	0.021 6	0.055 4	0.001 6	357	69	349	16	348	10	0.59
21NJ1-111	0.055 6	0.002 1	0.273 6	0.010 6	0.035 7	0.000 9	435	43	246	8	226	6	0.52
21NJ1-112	0.052 8	0.003 5	0.191 4	0.012 5	0.026 2	0.000 8	322	94	178	11	167	5	0.70
21NJ1-113	0.055 1	0.002 1	0.422 6	0.016 6	0.055 6	0.001 5	414	44	358	12	349	9	0.55
21NJ1-114	0.051 1	0.002 8	0.259 0	0.014 1	0.036 7	0.001 0	244	74	234	11	233	6	0.72
21NJ5-1-1	0.053 5	0.003 7	0.350 2	0.024 1	0.047 5	0.001 5	352	98	305	18	299	9	0.43
21NJ5-1-2	0.053 0	0.001 7	0.357 6	0.012 8	0.049 0	0.001 3	330	38	310	10	308	8	0.51
21NJ5-1-3	0.053 1	0.002 4	0.358 2	0.016 5	0.049 0	0.001 4	332	56	311	12	308	8	0.46
21NJ5-1-4	0.052 9	0.001 9	0.353 8	0.013 8	0.048 6	0.001 3	324	44	308	10	306	8	0.49
21NJ5-1-5	0.058 0	0.002 3	0.677 0	0.027 9	0.084 7	0.002 4	529	46	525	17	524	14	0.30
21NJ5-1-6	0.052 9	0.003 0	0.344 1	0.019 6	0.047 2	0.001 4	323	76	300	15	297	9	0.44
21NJ5-1-7	0.052 6	0.002 5	0.345 8	0.016 7	0.047 8	0.001 4	309	61	302	13	301	8	0.49
21NJ5-1-8	0.053 0	0.003 1	0.382 4	0.022 4	0.052 3	0.001 6	330	79	329	16	329	10	0.36
21NJ5-1-9	0.052 6	0.002 1	0.366 8	0.015 2	0.050 6	0.001 4	313	48	317	11	318	9	0.44
21NJ5-1-10	0.052 9	0.002 2	0.359 8	0.015 5	0.049 3	0.001 4	326	51	312	12	310	8	0.35
21NJ5-1-11	0.053 5	0.004 0	0.385 2	0.028 8	0.052 3	0.001 7	348	110	331	21	329	11	0.68
21NJ5-1-12	0.053 2	0.002 6	0.377 4	0.019 0	0.051 5	0.001 5	337	64	325	14	324	9	0.43
21NJ5-1-13	0.052 8	0.002 5	0.351 9	0.016 9	0.048 4	0.001 4	318	60	306	13	305	8	0.47
21NJ5-1-14	0.051 1	0.003 3	0.276 1	0.017 7	0.039 2	0.001 2	244	91	248	14	248	7	0.73
21NJ5-1-15	0.052 4	0.002 8	0.343 0	0.018 5	0.047 5	0.001 4	304	71	299	14	299	8	0.44
21NJ5-1-16	0.052 4	0.002 1	0.350 0	0.014 6	0.048 5	0.001 3	302	48	305	11	305	8	0.44
21NJ5-1-17	0.052 5	0.002 6	0.346 3	0.017 2	0.047 9	0.001 4	307	63	302	13	301	8	0.47
21NJ5-1-18	0.052 4	0.002 5	0.348 6	0.016 9	0.048 3	0.001 4	304	61	304	13	304	8	0.42
21NJ5-1-19	0.052 1	0.004 3	0.267 6	0.021 7	0.037 3	0.001 3	288	124	241	17	236	8	0.74
21NJ5-1-20	0.051 7	0.002 0	0.337 9	0.013 6	0.047 4	0.001 3	271	47	296	10	299	8	0.49
21NJ5-1-21	0.052 9	0.002 0	0.346 2	0.013 5	0.047 5	0.001 3	325	44	302	10	299	8	0.78
21NJ5-1-22	0.052 9	0.002 9	0.363 6	0.020 3	0.049 9	0.001 5	323	75	315	15	314	9	0.44
21NJ5-1-23	0.052 8	0.002 4	0.371 3	0.017 3	0.051 0	0.001 4	319	57	321	13	321	9	0.52
21NJ5-1-24	0.052 6	0.002 6	0.353 8	0.017 7	0.048 8	0.001 4	311	64	308	13	307	9	0.44
21NJ5-1-25	0.052 3	0.002 3	0.339 3	0.015 5	0.047 1	0.001 3	297	56	297	12	297	8	0.32
21NJ5-1-26	0.052 8	0.001 9	0.350 9	0.013 4	0.048 2	0.001 3	321	43	305	10	303	8	0.44
21NJ5-1-27	0.053 0	0.002 1	0.360 0	0.015 0	0.049 2	0.001 3	330	48	312	11	310	8	0.37
21NJ5-1-28	0.053 0	0.002 0	0.366 1	0.014 3	0.050 1	0.001 4	328	44	317	11	315	8	0.35
21NJ5-1-29	0.053 1	0.002 0	0.359 9	0.014 3	0.049 2	0.001 3	331	45	312	11	310	8	0.44
21NJ5-1-30	0.053 1	0.002 5	0.360 6	0.017 0	0.049 3	0.001 4	332	58	313	13	310	8	0.47
21NJ5-1-31	0.052 4	0.002 1	0.339 5	0.014 3	0.047 0	0.001 3	303	50	297	11	296	8	0.53
21NJ5-1-32	0.052 6	0.002 5	0.349 2	0.017 2	0.048 2	0.001 4	310	62	304	13	303	8	0.50
21NJ5-1-33	0.052 7	0.002 9	0.347 8	0.019 1	0.047 9	0.001 4	317	73	303	14	301	9	0.46

(continued Table 2)

No.	Isotopic ratio						Age/Ma						Th/U
	$^{207}\text{Pb}/^{206}\text{Pb}$	1 $\sigma$	$^{207}\text{Pb}/^{235}\text{U}$	1 $\sigma$	$^{206}\text{Pb}/^{238}\text{U}$	1 $\sigma$	$^{207}\text{Pb}/^{206}\text{Pb}$	1 $\sigma$	$^{207}\text{Pb}/^{235}\text{U}$	1 $\sigma$	$^{206}\text{Pb}/^{238}\text{U}$	1 $\sigma$	
21NJ5-1-34	0.052 5	0.001 9	0.351 9	0.013 3	0.048 6	0.001 3	309	42	306	10	306	8	0.39
21NJ5-1-35	0.052 6	0.001 9	0.335 4	0.012 8	0.046 2	0.001 2	313	43	294	10	291	8	0.62
21NJ5-1-36	0.052 2	0.002 2	0.345 2	0.015 2	0.048 0	0.001 3	294	53	301	11	302	8	0.46
21NJ5-1-37	0.052 6	0.002 6	0.372 1	0.018 8	0.051 3	0.001 5	313	65	321	14	322	9	0.39
21NJ5-1-38	0.052 5	0.001 9	0.356 7	0.013 9	0.049 3	0.001 3	307	44	310	10	310	8	0.43
21NJ5-1-39	0.053 3	0.004 9	0.384 8	0.034 9	0.052 4	0.001 9	342	140	331	26	329	12	0.43
21NJ5-1-40	0.052 8	0.002 0	0.357 1	0.014 0	0.049 0	0.001 3	322	45	310	10	308	8	0.45
21NJ5-1-41	0.050 8	0.002 9	0.257 0	0.014 9	0.036 7	0.001 1	230	80	232	12	232	7	0.99
21NJ5-1-42	0.052 1	0.003 1	0.338 9	0.020 2	0.047 2	0.001 4	288	83	296	15	297	9	0.44
21NJ5-1-43	0.052 5	0.002 9	0.336 9	0.018 9	0.046 5	0.001 4	308	76	295	14	293	8	0.47
21NJ5-1-44	0.052 7	0.001 7	0.342 4	0.012 1	0.047 1	0.001 2	316	38	299	9	297	8	0.42
21NJ5-1-45	0.052 7	0.001 8	0.351 5	0.013 0	0.048 4	0.001 3	314	41	306	10	305	8	0.58
21NJ5-1-46	0.052 6	0.002 0	0.365 8	0.014 4	0.050 4	0.001 4	311	45	317	11	317	8	0.40
21NJ5-1-47	0.052 4	0.002 5	0.344 9	0.016 8	0.047 7	0.001 3	303	62	301	13	301	8	0.36
21NJ5-1-48	0.052 7	0.002 4	0.350 2	0.016 1	0.048 2	0.001 3	315	57	305	12	303	8	0.42
21NJ5-1-49	0.052 4	0.003 8	0.334 7	0.023 9	0.046 3	0.001 5	303	105	293	18	292	9	0.56
21NJ5-1-50	0.054 6	0.002 8	0.363 0	0.019 0	0.048 2	0.001 4	397	68	314	14	303	8	0.42
21NJ5-1-51	0.052 5	0.002 7	0.343 5	0.018 0	0.047 5	0.001 4	306	69	300	14	299	8	0.36
21NJ5-1-52	0.052 9	0.001 8	0.353 6	0.013 0	0.048 5	0.001 3	324	40	307	10	305	8	0.61
21NJ5-1-53	0.052 8	0.002 1	0.335 1	0.013 7	0.046 0	0.001 2	321	47	293	10	290	8	0.93
21NJ5-1-54	0.052 8	0.002 4	0.354 2	0.016 7	0.048 7	0.001 3	320	59	308	13	306	8	0.58
21NJ5-1-55	0.052 9	0.002 4	0.355 6	0.016 4	0.048 8	0.001 3	322	57	309	12	307	8	0.49
21NJ5-1-56	0.052 3	0.001 8	0.329 7	0.012 4	0.045 8	0.001 2	297	42	289	9	288	7	0.40
21NJ5-1-57	0.052 8	0.001 7	0.357 3	0.012 7	0.049 1	0.001 3	321	39	310	10	309	8	0.51
21NJ5-1-58	0.052 7	0.003 3	0.357 6	0.022 3	0.049 3	0.001 5	314	88	310	17	310	9	0.64
21NJ5-1-59	0.051 1	0.002 5	0.267 8	0.013 1	0.038 0	0.001 1	247	63	241	10	240	7	0.52
21NJ5-1-60	0.051 1	0.015 6	0.130 6	0.039 5	0.018 5	0.001 0	245	454	125	35	118	6	0.69
21NJ5-1-61	0.055 5	0.001 7	0.335 7	0.010 6	0.043 9	0.001 0	433	34	294	8	277	6	0.83
21NJ5-1-62	0.054 7	0.006 0	0.263 2	0.028 2	0.034 9	0.001 3	400	176	237	23	221	8	0.06
21NJ5-1-63	0.057 5	0.003 4	0.350 9	0.020 3	0.044 2	0.001 2	512	80	305	15	279	7	0.46
21NJ5-1-64	0.058 8	0.004 1	0.441 7	0.030 4	0.054 5	0.001 6	561	99	371	21	342	10	0.81
21NJ5-1-65	0.057 9	0.002 7	0.382 4	0.017 9	0.047 9	0.001 2	527	59	329	13	301	8	0.36
21NJ5-1-66	0.054 7	0.001 7	0.336 4	0.011 0	0.044 6	0.001 1	400	35	294	8	281	6	0.68
21NJ5-1-67	0.049 7	0.002 9	0.133 8	0.007 7	0.019 6	0.000 5	179	85	127	7	125	3	0.05
21NJ6-1-1	0.056 9	0.005 1	0.396 8	0.033 5	0.050 6	0.001 5	486	204	339	24	318	9	0.45
21NJ6-1-2	0.052 7	0.003 0	0.362 9	0.020 4	0.049 9	0.001 4	316	77	314	15	314	9	0.41
21NJ6-1-3	0.052 1	0.002 2	0.329 7	0.014 3	0.045 9	0.001 2	288	53	289	11	289	7	0.48
21NJ6-1-4	0.052 1	0.003 5	0.342 0	0.022 5	0.047 6	0.001 4	289	96	299	17	300	9	0.46
21NJ6-1-5	0.052 2	0.002 0	0.334 3	0.013 4	0.046 5	0.001 2	294	47	293	10	293	7	0.59
21NJ6-1-6	0.051 4	0.004 0	0.348 3	0.025 4	0.049 2	0.001 3	258	178	303	19	309	8	0.54
21NJ6-1-7	0.056 9	0.003 1	0.369 2	0.020 3	0.047 1	0.001 3	486	72	319	15	297	8	0.51
21NJ6-1-8	0.053 0	0.002 0	0.357 2	0.014 3	0.048 9	0.001 3	328	47	310	11	308	8	0.41
21NJ6-1-9	0.055 3	0.002 4	0.359 2	0.015 7	0.047 1	0.001 3	423	52	312	12	297	8	0.55
21NJ6-1-10	0.053 1	0.001 9	0.363 6	0.013 9	0.049 7	0.001 3	333	43	315	10	312	8	0.45
21NJ6-1-11	0.052 8	0.001 8	0.352 3	0.012 5	0.048 4	0.001 2	318	39	306	9	305	8	0.49
21NJ6-1-12	0.052 8	0.001 6	0.347 2	0.011 6	0.047 7	0.001 2	320	36	303	9	300	7	0.47
21NJ6-1-13	0.052 8	0.001 6	0.347 2	0.011 3	0.047 7	0.001 2	322	34	303	8	300	7	0.38
21NJ6-1-14	0.057 7	0.002 4	0.409 9	0.017 2	0.051 5	0.001 4	519	48	349	12	324	8	0.44
21NJ6-1-15	0.053 1	0.001 9	0.356 2	0.013 5	0.048 7	0.001 3	333	43	309	10	306	8	0.46

(continued Table 2)

No.	Isotopic ratio						Age/Ma						Th/U
	$^{207}\text{Pb}/^{206}\text{Pb}$	1 $\sigma$	$^{207}\text{Pb}/^{235}\text{U}$	1 $\sigma$	$^{206}\text{Pb}/^{238}\text{U}$	1 $\sigma$	$^{207}\text{Pb}/^{206}\text{Pb}$	1 $\sigma$	$^{207}\text{Pb}/^{235}\text{U}$	1 $\sigma$	$^{206}\text{Pb}/^{238}\text{U}$	1 $\sigma$	
21NJ6-1-16	0.055 5	0.002 3	0.365 2	0.015 2	0.047 8	0.001 3	431	49	316	11	301	8	0.39
21NJ6-1-17	0.051 4	0.004 5	0.337 2	0.028 3	0.047 6	0.001 3	258	202	295	21	300	8	0.43
21NJ6-1-18	0.052 2	0.001 6	0.351 9	0.011 5	0.048 9	0.001 2	295	35	306	9	308	8	0.48
21NJ6-1-19	0.052 4	0.002 1	0.335 1	0.013 7	0.046 4	0.001 2	303	48	293	10	292	7	0.48
21NJ6-1-20	0.052 8	0.001 6	0.354 8	0.011 3	0.048 7	0.001 2	320	33	308	8	307	7	0.47
21NJ6-1-21	0.054 6	0.004 5	0.341 9	0.026 4	0.045 4	0.001 3	395	188	299	20	286	8	0.40
21NJ6-1-22	0.052 4	0.001 9	0.344 6	0.013 0	0.047 8	0.001 2	301	43	301	10	301	8	0.45
21NJ6-1-23	0.052 8	0.002 1	0.352 7	0.014 5	0.048 5	0.001 3	318	49	307	11	305	8	0.46
21NJ6-1-24	0.057 0	0.002 8	0.382 1	0.019 1	0.048 7	0.001 3	490	63	329	14	306	8	0.59
21NJ6-1-25	0.051 4	0.003 6	0.328 5	0.021 0	0.046 3	0.001 2	260	159	288	16	292	8	0.36
21NJ6-1-26	0.051 8	0.003 6	0.335 5	0.021 9	0.047 0	0.001 3	278	162	294	17	296	8	0.43
21NJ6-1-27	0.051 3	0.003 9	0.340 5	0.024 2	0.048 1	0.001 3	256	174	298	18	303	8	0.46
21NJ6-1-28	0.054 3	0.004 5	0.331 3	0.026 0	0.044 2	0.001 2	384	191	291	20	279	7	0.65
21NJ6-1-29	0.052 3	0.004 5	0.342 2	0.028 0	0.047 5	0.001 3	297	197	299	21	299	8	0.65
21NJ6-1-30	0.052 9	0.002 2	0.359 2	0.015 5	0.049 3	0.001 3	323	52	312	12	310	8	0.36
21NJ6-1-31	0.053 7	0.002 8	0.363 4	0.019 0	0.049 1	0.001 4	357	69	315	14	309	8	0.43
21NJ6-1-32	0.052 3	0.002 2	0.353 9	0.015 0	0.049 1	0.001 3	299	51	308	11	309	8	0.47
21NJ6-1-33	0.051 9	0.001 6	0.327 6	0.010 7	0.045 8	0.001 2	281	35	288	8	289	7	0.50
21NJ6-1-34	0.053 3	0.001 7	0.343 3	0.011 6	0.046 7	0.001 2	340	36	300	9	294	7	0.37
21NJ6-1-35	0.055 0	0.001 8	0.342 6	0.011 7	0.045 2	0.001 1	413	36	299	9	285	7	0.39
21NJ6-1-36	0.057 0	0.002 8	0.394 8	0.019 2	0.050 3	0.001 4	490	61	338	14	316	8	0.48
21NJ6-1-37	0.054 9	0.001 6	0.376 5	0.011 9	0.049 7	0.001 2	410	32	324	9	313	8	0.35
21NJ6-1-38	0.053 2	0.004 2	0.371 6	0.027 5	0.050 7	0.001 4	337	182	321	20	319	8	0.42
21NJ6-1-39	0.052 1	0.001 5	0.346 5	0.010 9	0.048 2	0.001 2	291	33	302	8	304	7	0.38
21NJ6-1-40	0.054 5	0.002 0	0.354 4	0.013 5	0.047 2	0.001 2	391	43	308	10	297	7	0.61
21NJ6-1-41	0.051 1	0.004 2	0.324 8	0.025 2	0.046 1	0.001 2	247	188	286	19	290	8	0.45
21NJ6-1-42	0.052 8	0.001 8	0.353 4	0.012 4	0.048 6	0.001 2	318	39	307	9	306	8	0.41
21NJ6-1-43	0.052 4	0.003 3	0.325 5	0.020 3	0.045 1	0.001 3	302	90	286	16	284	8	0.69
21NJ6-1-44	0.054 2	0.002 0	0.330 4	0.012 5	0.044 2	0.001 1	378	42	290	10	279	7	0.42
21NJ6-1-45	0.052 6	0.001 8	0.330 3	0.011 8	0.045 6	0.001 2	310	40	290	9	287	7	0.48
21NJ6-1-46	0.053 0	0.003 1	0.367 0	0.021 2	0.050 2	0.001 4	328	80	317	16	316	9	0.48
21NJ6-1-47	0.052 0	0.003 6	0.338 2	0.021 5	0.047 2	0.001 2	286	159	296	16	297	8	0.42
21NJ6-1-48	0.052 1	0.002 2	0.344 0	0.014 6	0.047 9	0.001 3	288	51	300	11	302	8	0.21
21NJ6-1-49	0.057 6	0.006 5	0.368 0	0.040 2	0.046 3	0.001 3	514	256	318	30	292	8	0.41
21NJ6-1-50	0.052 2	0.001 8	0.320 9	0.011 4	0.044 6	0.001 1	295	39	283	9	281	7	0.35
21NJ6-1-51	0.054 2	0.001 7	0.356 1	0.012 1	0.047 7	0.001 2	378	36	309	9	300	7	0.38
21NJ6-1-52	0.052 7	0.001 4	0.337 0	0.010 1	0.046 4	0.001 2	314	31	295	8	292	7	0.47
21NJ6-1-53	0.053 0	0.002 0	0.353 4	0.014 1	0.048 3	0.001 3	330	47	307	11	304	8	0.47
21NJ6-1-54	0.051 1	0.002 1	0.325 8	0.013 9	0.046 2	0.001 2	246	52	286	11	291	7	0.44
21NJ6-1-55	0.053 9	0.001 8	0.345 1	0.012 4	0.046 4	0.001 2	366	39	301	9	293	7	0.38
21NJ6-1-56	0.047 8	0.002 5	0.245 6	0.013 2	0.037 2	0.001 1	90	70	223	11	235	7	0.82
21NJ6-1-57	0.053 8	0.004 8	0.185 9	0.016 3	0.025 0	0.000 9	363	134	173	14	159	6	1.59
21NJ6-1-58	0.048 7	0.010 7	0.176 1	0.038 5	0.026 2	0.001 1	133	335	165	33	167	7	3.57
21NJ6-1-59	0.048 0	0.012 2	0.137 5	0.034 0	0.020 8	0.001 3	97	339	131	30	133	8	1.43
21NJ6-1-60	0.056 2	0.003 2	0.352 4	0.020 5	0.045 4	0.001 4	461	76	307	15	286	9	0.63
21NJ6-1-61	0.045 9	0.008 3	0.117 9	0.020 8	0.018 6	0.000 9	—	249	113	19	119	6	1.16
21NJ6-1-62	0.055 7	0.004 7	0.259 6	0.021 5	0.033 8	0.001 2	440	123	234	17	214	7	1.28
21NJ6-1-63	0.048 5	0.013 1	0.131 3	0.034 7	0.019 6	0.001 3	125	371	125	31	125	8	0.80
21NJ6-1-64	0.046 9	0.010 1	0.118 9	0.025 2	0.018 4	0.001 0	42	301	114	23	118	6	1.45

(continued Table 2)

No.	Isotopic ratio						Age/Ma						Th/U
	$^{207}\text{Pb}/^{206}\text{Pb}$	1 $\sigma$	$^{207}\text{Pb}/^{235}\text{U}$	1 $\sigma$	$^{206}\text{Pb}/^{238}\text{U}$	1 $\sigma$	$^{207}\text{Pb}/^{206}\text{Pb}$	1 $\sigma$	$^{207}\text{Pb}/^{235}\text{U}$	1 $\sigma$	$^{206}\text{Pb}/^{238}\text{U}$	1 $\sigma$	
21NJ6-1-65	0.050 6	0.009 1	0.129 7	0.022 8	0.018 6	0.000 9	220	283	124	21	119	6	1.01
21NJ6-1-66	0.048 3	0.011 0	0.121 1	0.026 9	0.018 2	0.001 1	113	313	116	24	116	7	1.49
21NJ6-1-67	0.045 3	0.009 2	0.116 6	0.023 1	0.018 7	0.000 9	—	266	112	21	119	6	1.85
21NJ6-1-68	0.056 6	0.003 1	0.319 5	0.017 8	0.041 0	0.001 2	476	72	281	14	259	7	0.79
21NJ6-1-69	0.056 0	0.003 0	0.391 9	0.021 5	0.050 8	0.001 5	452	72	336	16	320	9	1.45
21NJ6-1-70	0.052 9	0.005 9	0.132 5	0.014 3	0.018 2	0.000 7	325	173	126	13	116	4	1.82
21NJ6-1-71	0.048 0	0.013 1	0.122 2	0.032 4	0.018 5	0.001 4	99	358	117	29	118	9	1.30
21NJ6-1-72	0.052 5	0.011 7	0.141 5	0.030 7	0.019 6	0.001 2	306	339	134	27	125	7	0.82
21NJ6-1-73	0.045 1	0.006 9	0.116 6	0.017 4	0.018 8	0.000 8	—	216	112	16	120	5	1.61
21NJ6-1-74	0.050 9	0.005 5	0.131 1	0.013 8	0.018 7	0.000 7	236	169	125	12	119	4	1.01
21NJ6-1-75	0.049 1	0.005 6	0.126 2	0.014 1	0.018 7	0.000 7	154	181	121	13	119	4	1.67
21NJ6-1-76	0.050 6	0.008 6	0.130 2	0.021 5	0.018 7	0.000 9	220	274	124	19	120	6	1.61
21NJ6-1-77	0.049 9	0.005 0	0.263 1	0.025 9	0.038 3	0.001 3	192	158	237	21	242	8	0.42
21NJ6-1-78	0.055 7	0.005 5	0.279 4	0.026 7	0.036 5	0.001 3	441	149	250	21	231	8	1.56
21NJ6-1-79	0.054 7	0.003 1	0.363 2	0.018 6	0.048 1	0.001 2	401	132	315	14	303	7	0.31
21NJ6-1-80	0.045 8	0.004 0	0.258 9	0.022 6	0.041 1	0.001 3	—	132	234	18	260	8	0.50
21NJ6-1-81	0.050 2	0.005 2	0.265 0	0.026 6	0.038 3	0.001 1	204	235	239	21	242	7	0.70
21NJ6-1-82	0.051 7	0.010 7	0.131 0	0.026 4	0.018 5	0.001 1	272	312	125	24	118	7	1.09
21NJ6-1-83	0.056 0	0.003 9	0.271 8	0.018 5	0.035 3	0.001 1	452	96	244	15	224	7	0.90
21NJ6-1-84	0.049 4	0.009 5	0.127 7	0.023 9	0.018 8	0.001 0	167	286	122	22	120	6	1.08
21NJ6-1-85	0.051 2	0.011 2	0.136 4	0.029 3	0.019 3	0.000 8	252	405	130	26	123	5	1.56
21NJ6-1-86	0.046 5	0.006 9	0.164 7	0.023 9	0.025 8	0.001 1	24	221	155	21	164	7	1.47
21NJ6-1-87	0.055 5	0.003 0	0.278 9	0.015 1	0.036 6	0.001 0	432	73	250	12	232	6	0.88
21NJ6-1-88	0.051 5	0.006 2	0.131 0	0.015 4	0.018 5	0.000 7	263	195	125	14	118	4	2.27
21NJ6-1-89	0.044 1	0.007 4	0.110 6	0.018 2	0.018 3	0.000 9	—	216	107	17	117	6	1.52
21NJ6-1-90	0.046 5	0.008 1	0.117 5	0.020 0	0.018 4	0.000 9	24	249	113	18	118	6	1.52
21NJ8-1	0.049 3	0.005 9	0.125 8	0.014 6	0.018 5	0.000 7	164	189	120	13	118	5	1.06
21NJ8-2	0.048 6	0.002 6	0.125 2	0.006 8	0.018 7	0.000 5	127	74	120	6	120	3	2.17
21NJ8-3	0.049 7	0.005 4	0.126 1	0.013 3	0.018 4	0.000 7	181	168	121	12	118	4	1.19
21NJ8-4	0.052 9	0.002 8	0.363 5	0.019 5	0.049 9	0.001 4	325	71	315	15	314	9	0.74
21NJ8-5	0.050 1	0.011 5	0.129 9	0.029 0	0.018 8	0.001 2	201	324	124	26	120	7	0.89
21NJ8-6	0.049 0	0.005 1	0.120 0	0.012 2	0.017 8	0.000 6	146	162	115	11	114	4	1.33
21NJ8-7	0.049 2	0.009 8	0.126 9	0.024 7	0.018 7	0.001 0	158	300	121	22	119	6	1.00
21NJ8-8	0.049 2	0.005 2	0.122 2	0.012 7	0.018 0	0.000 7	157	165	117	12	115	4	2.56
21NJ8-9	0.053 2	0.002 7	0.377 3	0.019 2	0.051 5	0.001 4	337	66	325	14	324	9	0.36
21NJ8-10	0.052 1	0.010 4	0.136 9	0.026 6	0.019 1	0.001 1	289	308	130	24	122	7	0.80
21NJ8-11	0.049 4	0.003 4	0.125 7	0.008 7	0.018 5	0.000 6	166	102	120	8	118	4	1.72
21NJ8-12	0.046 1	0.007 5	0.114 4	0.018 2	0.018 0	0.000 7	—	287	110	17	115	4	1.05
21NJ8-13	0.048 9	0.004 2	0.122 6	0.010 5	0.018 2	0.000 6	143	131	117	9	116	4	1.39
21NJ8-14	0.048 9	0.003 4	0.119 5	0.008 3	0.017 7	0.000 5	142	102	115	8	113	3	1.72
21NJ8-15	0.049 3	0.005 7	0.131 9	0.014 9	0.019 4	0.000 7	162	183	126	13	124	5	0.60
21NJ8-16	0.048 1	0.002 4	0.122 0	0.006 2	0.018 4	0.000 5	103	67	117	6	118	3	0.87
21NJ8-17	0.052 6	0.006 1	0.413 7	0.046 6	0.057 1	0.001 8	310	264	351	33	358	11	0.81
21NJ8-18	0.047 3	0.003 2	0.119 0	0.007 9	0.018 3	0.000 5	66	93	114	7	117	3	1.12
21NJ8-19	0.052 4	0.003 7	0.126 9	0.008 8	0.017 6	0.000 5	305	102	121	8	112	3	1.37
21NJ8-20	0.051 2	0.003 1	0.207 2	0.012 6	0.029 4	0.000 9	249	86	191	11	187	5	2.00
21NJ8-21	0.047 9	0.005 9	0.124 5	0.015 0	0.018 9	0.000 8	93	195	119	14	120	5	0.98
21NJ8-22	0.048 9	0.004 6	0.126 0	0.011 7	0.018 7	0.000 6	143	146	120	11	119	4	1.05
21NJ8-23	0.049 1	0.002 8	0.124 5	0.007 2	0.018 4	0.000 5	151	82	119	6	118	3	1.43

(continued Table 2)

No.	Isotopic ratio						Age/Ma						Th/U
	$^{207}\text{Pb}/^{206}\text{Pb}$	1 $\sigma$	$^{207}\text{Pb}/^{235}\text{U}$	1 $\sigma$	$^{206}\text{Pb}/^{238}\text{U}$	1 $\sigma$	$^{207}\text{Pb}/^{206}\text{Pb}$	1 $\sigma$	$^{207}\text{Pb}/^{235}\text{U}$	1 $\sigma$	$^{206}\text{Pb}/^{238}\text{U}$	1 $\sigma$	
21NJ8-24	0.048 4	0.003 5	0.120 2	0.008 7	0.018 0	0.000 6	118	106	115	8	115	3	1.35
21NJ8-25	0.050 2	0.004 2	0.122 8	0.010 1	0.017 8	0.000 6	204	128	118	9	113	4	0.98
21NJ8-26	0.050 3	0.003 5	0.128 5	0.008 8	0.018 5	0.000 6	211	103	123	8	118	4	0.78
21NJ8-27	0.047 9	0.003 8	0.123 6	0.009 5	0.018 7	0.000 6	93	114	118	9	120	4	1.18
21NJ8-28	0.051 5	0.004 5	0.206 8	0.017 8	0.029 1	0.001 0	262	135	191	15	185	6	0.67
21NJ8-29	0.049 7	0.007 2	0.169 7	0.024 2	0.024 8	0.001 0	179	240	159	21	158	6	0.79
21NJ8-30	0.052 9	0.003 2	0.343 5	0.020 6	0.047 1	0.001 4	325	84	300	16	297	8	1.20
21NJ8-31	0.049 5	0.002 8	0.129 1	0.007 3	0.018 9	0.000 5	173	79	123	7	121	3	1.89
21NJ8-32	0.049 8	0.004 0	0.124 1	0.009 9	0.018 1	0.000 6	187	122	119	9	115	4	1.03
21NJ8-33	0.054 5	0.003 6	0.376 0	0.024 5	0.050 1	0.001 5	390	93	324	18	315	9	0.62
21NJ8-34	0.049 0	0.012 5	0.137 4	0.034 1	0.020 3	0.001 3	148	354	131	30	130	8	0.88
21NJ8-35	0.051 0	0.002 1	0.229 6	0.009 9	0.032 6	0.000 9	243	53	210	8	207	5	0.49
21NJ8-36	0.049 6	0.006 7	0.129 2	0.017 1	0.018 9	0.000 8	178	221	123	15	121	5	0.93
21NJ8-37	0.052 5	0.003 4	0.342 4	0.022 2	0.047 3	0.001 4	307	94	299	17	298	9	0.72
21NJ8-38	0.049 6	0.008 7	0.120 4	0.020 6	0.017 6	0.000 9	178	271	115	19	112	6	0.86
21NJ8-39	0.049 4	0.002 5	0.125 1	0.006 5	0.018 4	0.000 5	166	71	120	6	117	3	1.69
21NJ8-40	0.052 7	0.003 5	0.334 3	0.022 2	0.046 1	0.001 4	314	97	293	17	290	9	0.80
21NJ8-41	0.048 0	0.003 5	0.125 1	0.009 1	0.018 9	0.000 6	97	106	120	8	121	4	2.08
21NJ8-42	0.050 0	0.010 8	0.135 0	0.028 2	0.019 6	0.001 1	197	321	129	25	125	7	1.06
21NJ8-43	0.049 2	0.004 0	0.120 9	0.009 7	0.017 8	0.000 6	157	122	116	9	114	4	1.67
21NJ8-44	0.049 8	0.012 9	0.129 4	0.032 6	0.018 9	0.001 3	186	360	124	29	120	8	0.78
21NJ8-45	0.046 1	0.005 8	0.112 3	0.013 5	0.017 7	0.000 6	—	239	108	12	113	4	0.60
21NJ8-46	0.053 1	0.002 9	0.335 7	0.018 4	0.045 9	0.001 3	331	75	294	14	289	8	0.52
21NJ8-47	0.050 2	0.003 6	0.189 3	0.013 3	0.027 4	0.000 8	203	106	176	11	174	5	0.71
21NJ8-48	0.049 1	0.003 7	0.121 5	0.009 1	0.017 9	0.000 6	155	112	116	8	115	3	0.91
21NJ8-49	0.050 5	0.002 5	0.127 5	0.006 4	0.018 3	0.000 5	216	67	122	6	117	3	0.89
21NJ8-50	0.053 2	0.004 7	0.129 7	0.011 2	0.017 7	0.000 6	338	136	124	10	113	4	0.51

Note: “—” indicates data missing due to experimental error.

For sample 21NJ6-1, 120 zircons were analyzed, yielding 90 with less than 10% discordance (Table 2). The  $^{206}\text{Pb}/^{238}\text{U}$  ages from 90 concordant zircon grains ranged from  $324\pm8$  Ma to  $116\pm4$  Ma (Fig.6c), with four groups: 324–279 Ma (58 grains, peak at 302 Ma), 260–214 Ma (9 grains, peak at 235 Ma), 167–159 Ma (3 grains, peak at 167 Ma) and 133–116 Ma (20 grains, peak at 118 Ma).

For sample 21NJ8, 60 zircons were analyzed, yielding 50 with less than 10% discordance (Table 2). The  $^{206}\text{Pb}/^{238}\text{U}$  ages from these grains ranged from  $358\pm11$  Ma to  $112\pm3$  Ma (Fig.6d), divided into three groups: 358–289 Ma (8 grains, peak at 296 Ma), 207–158 Ma (5 grains, peak at 183 Ma), and 130–112 Ma (37 grains, peak at 117 Ma).

## 5 Discussion

### 5.1 Depositional age of Jiufengshan Formation

Analyses of 370 detrital zircon grains of four sandstone samples from Jiufengshan Formation revealed that 321 grains yielded discordance between  $\leq 10\%$  and  $\geq -10\%$  (Table 2). The zircon ages ranged from  $875\pm20$  Ma to  $112\pm3$  Ma (Fig.7a), with significant populations: 875 Ma, 633 Ma, 524 Ma, 469 Ma, 374–259 Ma (193 grains, peaking at 296 Ma), 253–158 Ma (63 grains, peaking at 223 Ma and 176 Ma) and 133–112 Ma (61 grains, peaking at 117 Ma). The youngest detrital zircon U–Pb age often constrains the maximum depositional age of strata (Stewart *et al.*,

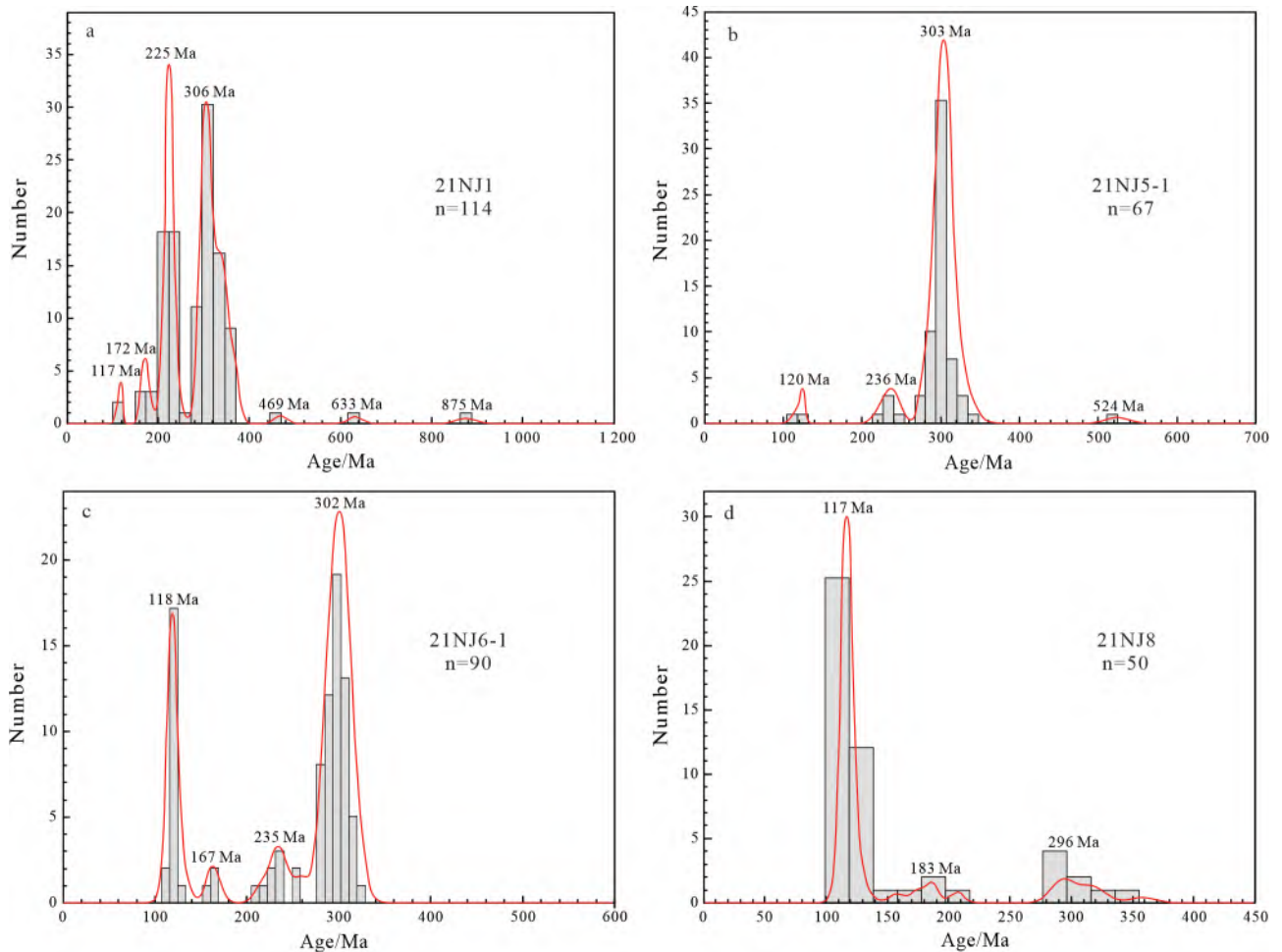


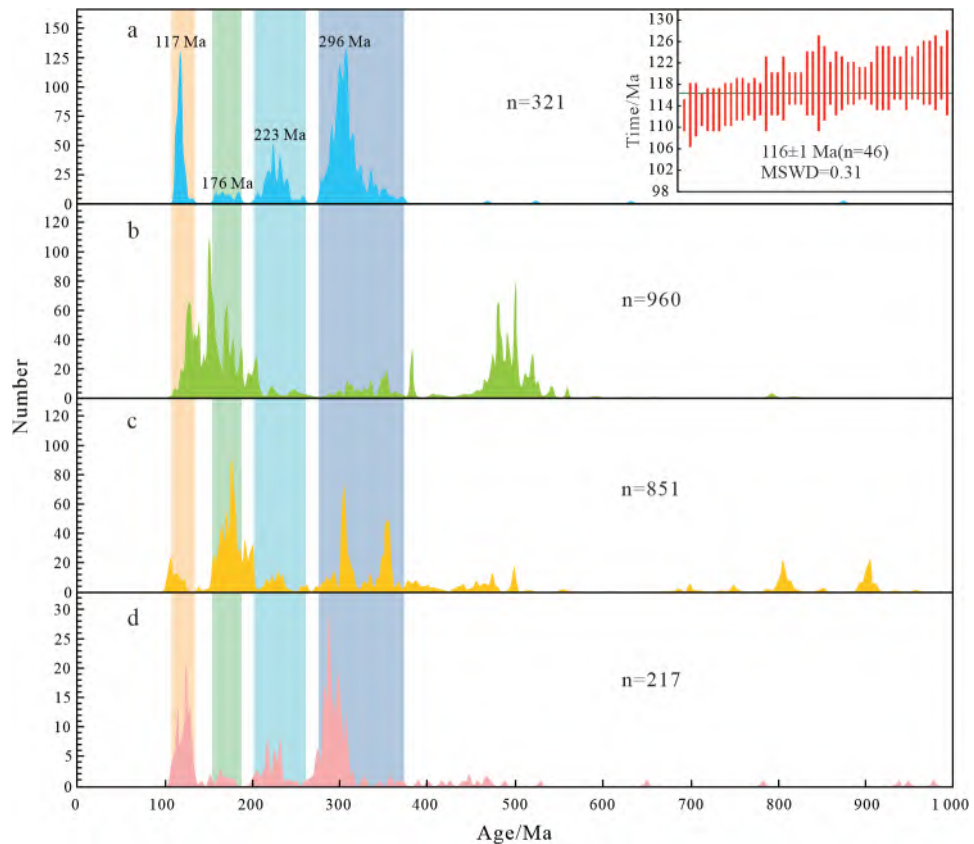
**Fig.6** Age distributions of detrital zircons in sandstones from Jiufengshan Formation

2001; Surpless *et al.*, 2006; Brown & Gehrels, 2007; Dickinson & Gehrels, 2009). A weighted average age of 46 detrital zircons within the  $1\sigma$  error range of the youngest zircon age indicates a maximum sedimentation age for the Jiufengshan Formation at  $116 \pm 1$  Ma (Fig.7a).

## 5.2 Provenance analysis

All sandstone samples from the Jiufengshan Formation are characterized by low compositional maturity, a high ratio of feldspar to lithic debris, low textural maturity, poor sorting, and low porosity (Fig.3), indicating proximity to the source and rapid denudation deposition. The detrital zircon exhibits angular to subangular shapes with poor rounding (Fig.5), further indicating a proximal accumulation.

Zircon age peak comparison is a common and effective method in provenance analysis (Chen *et al.*, 2022, 2024). Therefore, this study collected magmatic zircons from potential provenance areas of the Jiufengshan Formation (Miao *et al.*, 2003; Ge *et al.*, 2005; Liu *et al.*, 2008a; Yang & Wang, 2010; Zhao *et al.*, 2010; Zhang *et al.*, 2010; Wu *et al.*, 2011; She *et al.*, 2012; Li *et al.*, 2013b; Xu *et al.*, 2013; Miao *et al.*, 2015; Tang *et al.*, 2015; Dong *et al.*, 2016; Gao *et al.*, 2016; Liu *et al.*, 2017a; Wang *et al.*, 2017; Zhao *et al.*, 2017; Zhang *et al.*, 2018; Yang *et al.*, 2020; Li *et al.*, 2023a; Li *et al.*, 2023b; Li *et al.*, 2023c). As shown in Fig.7, the detrital zircon age peaks of the Jiufengshan Formation are essentially consistent with these magmatic zircon ages from the Longjiang, Guanghua and Jiufengshan formations. However, Cambrian zircons



(a) Detrital zircon U–Pb ages of Jiufengshan Formation; (b) magmatic zircon ages from the Da Hinggan Ling (Mts.); (c) magmatic zircon ages from the Xiao Hinggan Ling (Mts.); (d) volcanic rock ages of Longjiang, Guanghua and Jiufengshan formations.

**Fig.7 Histogram of detrital zircon U–Pb ages from Jiufengshan Formation compared with potential source areas**

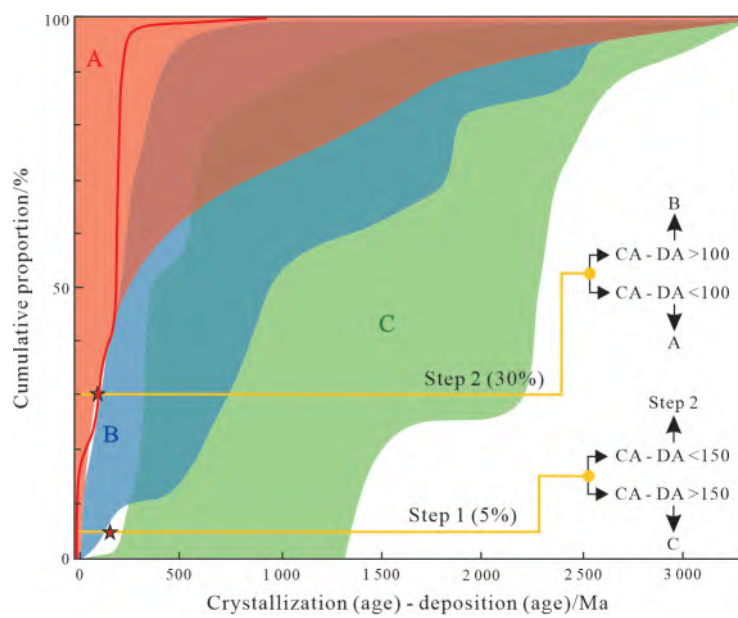
are significantly absent in the Jiufengshan Formation compared to the Da Hinggan Ling (Mts.) and the Xiao Hinggan Ling (Mts.). Consequently, these findings suggest that the source materials of the Jiufengshan Formation are derived from early-formed and contemporaneous volcanic rocks in the study area.

### 5.3 Tectonic implication

Zircon sources and transport processes determine the age distribution of detrital zircons in the strata, with peak age composition effectively reflecting the tectonic environment (Cawood *et al.*, 2012). The detrital zircons in the Jiufengshan Formation have a concentrated age distribution, with about 30% being less than 100 Ma from the sedimentary age (Fig.8; Table 2), indicating an intermediate tectonic setting between convergent and collisional basins.

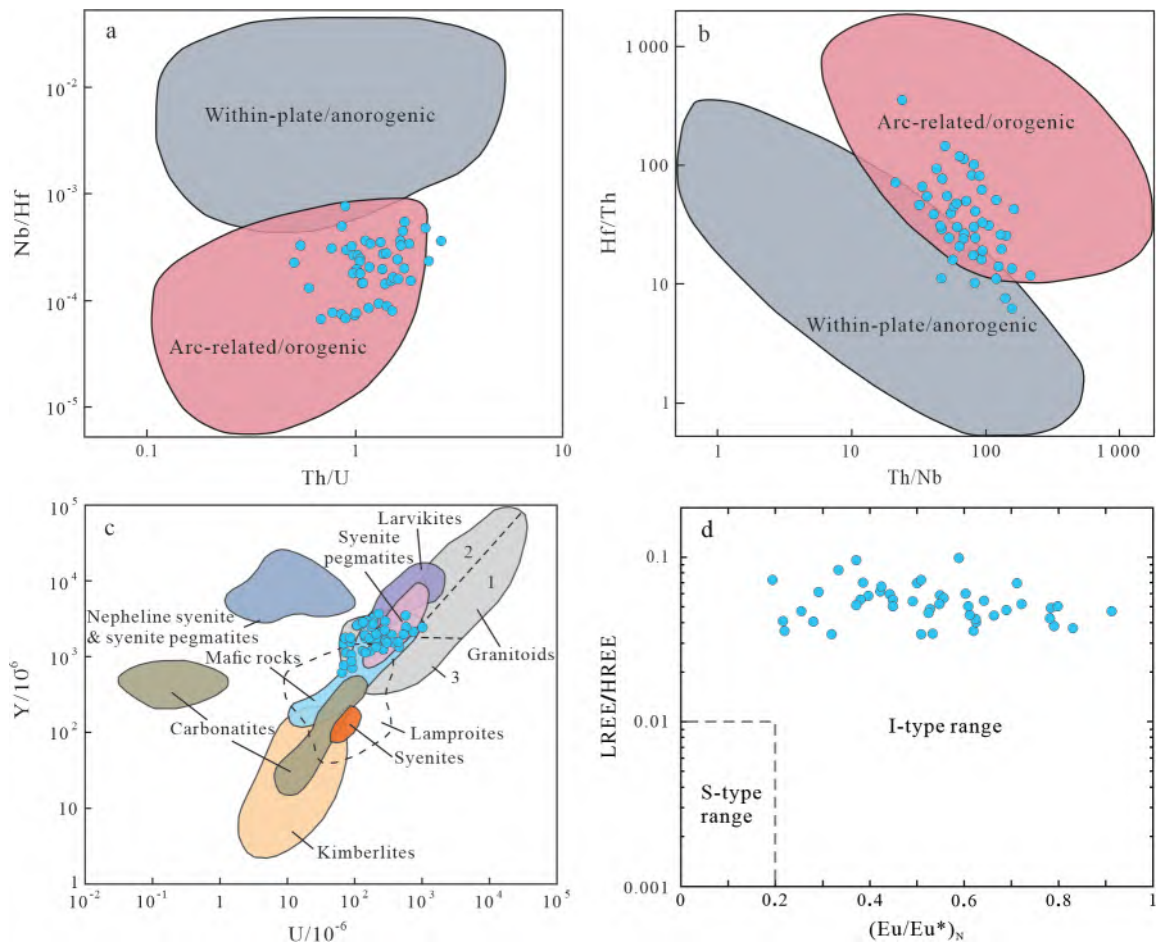
Analysis of these youngest detrital zircons from Early Cretaceous Jiufengshan Formation (120–112 Ma)

reveals their primary originate from a volcanic arc associated with orogenesis, as indicated by zircon tectonic setting discrimination diagrams (Fig.9a, b; Table 3). The zircon genesis discrimination diagram shows these zircons come from a high-silica granite source (Fig.9c; Table 3). Furthermore, the zircon genesis classification diagram identifies them as I-type granite zircons (Fig.9d; Table 3). The prevalence of I-type granites is typical of oceanic plates subduction, suggesting that the youngest detrital zircons in the Jiufengshan Formation are sourced from I-type granitic volcanic arcs associated with orogenesis, indicative of low-angle subduction of the Paleo-Pacific plate. Sandstone framework analysis places the sandstones from the Jiufengshan Formation within a transitional arc region (Fig.4). In the detrital zircon tectonic discrimination diagram, these detrital zircons fall at the boundary between subduction and collision basins (Fig.8). Collectively, the evidence suggests that during



A. Convergent basin; B. collisional basin; C. extensional basin.

**Fig.8 Detrital zircon tectonic discrimination diagram** (modified after Cawood *et al.*, 2012)



(a, b) Zircon tectonic setting discrimination diagrams; (c) zircon genesis discrimination diagram; (d) zircon genesis classification diagram.

**Fig.9 Zircon genesis and tectonic discrimination diagrams** (modified after Belousova *et al.*, 2002; Grimes *et al.*, 2007; Liu *et al.*, 2022)

**Table 3 Detrital zircon trace elements ( $10^6$ ) of Jiufengshan Formation**

No.	Y	Nb	La	Ce	Pr	Nd	Sm	Eu	Gd	Tb	Dy	Ho	Er	Tm	Yb	Lu	Hf	Th	U
21NJ1-69	1 046	4	2	18	1	6	5	1	29	9	97	35	155	31	295	55	6 060	85	88
21NJ1-80	1 904	6	7	37	1	5	7	1	29	12	156	63	302	66	661	130	8 949	193	352
21NJ5-1-60	434	1	3	18	1	5	3	1	9	3	35	14	63	14	146	29	8 493	24	35
21NJ6-1-61	1 456	1	1	23	0	4	7	4	31	11	125	50	224	47	478	95	6 546	79	68
21NJ6-1-64	1 774	1	0	28	1	8	12	6	46	15	167	61	266	57	568	111	6 163	120	84
21NJ6-1-65	861	1	0	25	0	2	2	1	17	6	69	28	130	30	311	62	7 343	90	89
21NJ6-1-66	2 611	2	1	50	1	10	18	8	70	23	252	92	386	84	792	149	6 896	168	112
21NJ6-1-67	1 741	2	1	56	0	3	7	3	40	13	159	60	260	54	516	96	6 777	260	140
21NJ6-1-70	3 687	5	6	117	2	19	17	9	88	30	353	125	534	107	1 017	189	7 114	406	223
21NJ6-1-71	1 760	1	0	26	0	3	10	4	39	12	150	56	258	56	534	105	5 832	94	72
21NJ6-1-73	2 816	2	0	59	0	7	13	6	59	22	254	96	428	88	823	159	6 553	211	130
21NJ6-1-74	1 756	3	0	51	0	4	8	2	34	12	147	58	266	58	583	113	7 774	173	170
21NJ6-1-75	3 218	5	1	99	1	8	15	7	84	27	299	111	473	97	927	170	6 624	319	193
21NJ6-1-76	2 995	3	1	80	0	4	9	6	61	23	270	101	444	91	880	165	6 188	251	156
21NJ6-1-82	1 547	2	0	39	0	3	6	4	30	11	130	50	230	52	505	100	7 270	95	87
21NJ6-1-84	1 179	2	0	37	0	3	4	2	18	8	96	39	183	41	420	86	7 201	143	132
21NJ6-1-88	1 948	3	0	68	3	5	12	4	50	16	183	68	287	60	559	105	6 442	473	209
21NJ6-1-89	2 591	2	0	61	0	9	12	7	60	21	231	87	377	78	774	140	6 276	189	124
21NJ6-1-90	2 592	1	0	47	1	12	21	8	77	24	249	89	378	78	742	140	6 956	163	108
21NJ8-1	1 976	4	0	59	0	5	11	4	44	15	179	69	300	63	616	116	8 050	147	139
21NJ8-2	2 442	8	18	175	6	32	18	5	68	21	240	84	367	76	732	140	7 867	1 264	577
21NJ8-3	1 888	6	0	75	0	4	6	2	35	13	157	63	295	65	654	130	8 598	278	234
21NJ8-5	697	1	0	29	0	2	4	1	13	5	58	25	111	25	255	51	8 307	82	91
21NJ8-6	2 525	5	0	66	0	5	10	4	54	18	224	87	384	81	773	148	6 926	236	177
21NJ8-7	770	1	0	26	0	2	5	1	22	7	71	26	117	24	239	47	7 753	69	69
21NJ8-8	2 722	4	0	216	1	9	19	8	95	28	292	100	397	75	663	123	5 355	480	185
21NJ8-11	1 504	3	0	47	0	3	5	2	25	10	131	50	232	49	501	99	7 643	649	376
21NJ8-12	1 652	4	0	61	0	3	7	2	34	12	141	58	261	57	579	116	8 657	220	208
21NJ8-13	1 321	2	0	33	0	3	4	2	24	9	113	44	208	47	462	91	7 319	287	206
21NJ8-14	1 965	11	0	119	0	4	7	2	39	15	174	66	298	63	612	118	9 377	913	526
21NJ8-16	2 121	11	1	75	0	3	5	2	31	13	170	69	336	74	758	150	10 372	636	734
21NJ8-18	2 055	6	3	70	1	5	6	2	31	12	159	67	323	74	752	156	7 912	321	286
21NJ8-19	1 867	4	1	53	1	5	6	2	31	12	151	61	282	63	626	130	7 255	379	276
21NJ8-21	1 772	3	2	55	1	5	7	2	37	12	151	60	275	60	590	119	8 622	155	158
21NJ8-22	1 160	3	0	54	0	2	3	1	21	8	99	38	179	39	396	80	8 678	182	172
21NJ8-23	1 526	5	0	70	0	2	5	2	29	10	132	51	229	50	495	98	8 923	629	443
21NJ8-24	1 598	3	0	45	0	2	4	2	25	10	124	52	247	55	561	114	7 828	395	291
21NJ8-25	2 076	4	0	45	0	2	5	2	29	12	166	69	325	74	758	158	7 469	246	250
21NJ8-26	1 540	6	0	40	0	2	5	1	24	9	129	53	247	55	556	111	9 557	246	317
21NJ8-27	1 495	3	0	31	0	2	4	1	23	9	114	48	230	52	536	109	7 447	246	209
21NJ8-32	2 156	4	0	47	0	2	4	2	33	12	173	71	340	76	752	154	7 448	279	270
21NJ8-38	1 140	1	12	44	4	20	9	2	29	9	102	38	166	35	332	66	7 556	64	74
21NJ8-39	3 399	7	1	106	1	10	20	6	86	28	313	115	505	109	1 066	212	7 446	979	577
21NJ8-43	2 935	5	0	83	0	7	13	6	63	23	263	99	440	92	870	171	7 511	464	279
21NJ8-44	617	1	0	16	0	1	2	1	12	5	52	19	98	22	234	49	7 230	50	64
21NJ8-45	1 122	2	1	16	0	3	7	1	28	9	106	38	172	35	337	65	8 073	86	143
21NJ8-48	1 305	6	0	75	0	1	4	1	21	8	102	42	202	46	458	93	9 911	410	450
21NJ8-49	2 387	19	0	113	0	3	6	1	42	16	204	79	368	79	762	142	10 023	894	1 002
21NJ8-50	1 235	4	0	29	0	1	3	2	20	8	97	38	182	43	436	92	8 968	135	264

the Jiufengshan Formation period, the northeastern Da Hinggan Ling (Mts.) likely functioned as a retro-arc basin associated with the low-angle subduction of the Paleo-Pacific plate (Li *et al.*, 2013a).

## 6 Conclusions

(1) New detrital zircon U–Pb ages indicate that the maximum depositional age of the Jiufengshan Formation is  $116 \pm 1$  Ma.

(2) Petrographic analysis and zircon age peak comparisons suggest that the sandstones from Jiufengshan Formation resulted from proximal deposition, sourced from early-formed and contemporaneous volcanic rocks within the study area.

(3) The trace element compositions and age distributions of detrital zircons, along with sandstone framework analysis, imply that the northeastern Da Hinggan Ling (Mts.) exhibited a retro-arc basin tectonic setting during the Jiufengshan Formation period, likely related to the low-angle subduction of the Paleo-Pacific plate.

## Author contributions

LIANG Chenyue: conceptualization, methodology, resources, validation and software. JIA Xianghe: validation, formal analysis, investigation, writing-original draft preparation, writingreview, editing and visualization. ZHENG Changqing: formal analysis, investigation and validation.

## Conflict of interest statement

The authors declare that they have no known competing financial interests or personal relationships that could have appeared to influence the work reported in this paper.

## References

- Andersen T. 2002. Correction of common lead in U-Pb analyses that do not report  $^{204}\text{Pb}$ . *Chemical Geology*, **192**(1/2): 59-79.
- Belousova E A, Griffin W L, O'Reilly S Y, et al. 2002. Igneous zircon: Trace element composition as an indicator of source rock type. *Contributions to Mineralogy and Petrology*, **143**(5): 602-622.
- Brown E R, Gehrels G E. 2007. Detrital zircon constraints on terrane ages and affinities and timing of orogenic events in the San Juan Islands and North Cascades, Washington. *Canadian Journal of Earth Sciences*, **44**: 1375-1396.
- Bruguier O, Lancelet J R. 1997. U-Pb dating on single detrital zircon grains from the Triassic Songpan-Ganze flysch (central China): Provenance and tectonic correlations. *Earth and Planetary Science Letters*, **152**: 217-231.
- Carter A, Steve J M. 1999. Combined detrital-zircon fission-track and U-Pb dating: A new approach to understanding hinterland evolution. *Geology*, **27**(3): 235-238.
- Cawood P A, Hawkesworth C J, Dhuime B. 2012. Detrital zircon record and tectonic setting. *Geology*, **40**: 875-878.
- Chen L, Liang C Y, Neubauer F, et al. 2022. Sedimentary processes and deformation styles of the Mesozoic sedimentary succession in the northern margin of the Mohe basin, NE China: Constraints on the final closure of the Mongol-Okhotsk Ocean. *Journal of Asian Earth Sciences*, **232**: 105052.
- Chen L, Liang C Y, Neubauer F, et al. 2024. A review on nature and multi-stage evolution of the Mongol-Okhotsk Ocean: New insights from the sedimentary record in the Mohe Basin. *Earth Science Reviews*, **254**: 104794.
- Cherniak D J, Watson E B. 2000. Pb diffusion in zircon. *Chemical Geology*, **172**: 5-24.
- Dickinson W R, Beard L S, Brakenridge G R, et al. 1983. Provenance of North American Phanerozoic sandstones in relation to tectonic setting. *Geological Society of America Bulletin*, **94**: 222-235.
- Dickinson W R, Gehrels G E. 2009. Use of U-Pb ages of detrital zircons to infer maximum depositional ages of strata: A test against a Colorado Plateau Mesozoic database. *Earth and Planetary Science Letters*, **288**(1/2): 115-125.
- Dong Y, Ge W C, Yang H, et al. 2016. Geochronology, geochemistry, and Hf isotopes of Jurassic intermediate-acidic intrusions in the Xing'an Block, northeastern China: Petrogenesis and implications for subduction of the Paleo-Pacific oceanic plate. *Journal of Asian Earth Sciences*, **118**: 11-31.
- Fedo C M, Sircombe K N, Rainbird R H. 2003. Detrital zircon analysis of the sedimentary record. *Reviews in Mineralogy and Geochemistry*, **53**: 277-303.
- Fu D, Huang B, Kusky T M, et al. 2018. A Middle Permian ophiolitic melange belt in the Solonker Suture Zone, western Inner Mongolia, China: Implications for the evolution of the Paleo-Asian Ocean. *Tectonics*, **37**: 1292-1320.
- Fu D, Huang B, Peng S B, et al. 2016. Geochronology and geochemistry of Late Carboniferous volcanic rocks from northern Inner Mongolia, North China: Petrogenesis and tectonic implications. *Gondwana Research*, **36**: 545-560.
- Gao F H, Wang L, Xu W L, et al. 2016. Age and provenance of the Late Paleozoic strata in Lesser Xing'an Range: Evidence from field geology and detrital zircon U-Pb ages. *Journal of Jilin University: Earth Science Edition*, **46**(2): 469-481. (in Chinese with English abstract)
- Garzanti E. 2019. Petrographic classification of sand and sandstone. *Earth-Science Reviews*, **192**: 545-563.

- Ge W C, Wu F Y, Zhou C Y, et al. 2005. Zircon U-Pb ages and its significance of the Mesozoic granites in the Wulanhaote region, central Da Hinggan Mountain. *Acta Petrologica Sinica*, **21**(3): 749-762. (in Chinese with English abstract)
- Griffin W L, Belousova E A, Shee S R, et al. 2004. Archean crustal evolution in the northern Yilgarn craton: U-Pb and Hf-isotope evidence from detrital zircons. *Precambrian Research*, **131**: 231-282.
- Grimes C B, John B E, Kelemen P B, et al. 2007. Trace element chemistry of zircons from oceanic crust: A method for distinguishing detrital zircon provenance. *Geology*, **35**(6): 643-646.
- Guan Q B, Liu Z H, Wang B, et al. 2018. Middle Jurassic-Early Cretaceous tectonic evolution of the Bayanhushuo area, southern Great Xing'an Range, NE China: Constraints from zircon U-Pb geochronological and geochemical data of volcanic and subvolcanic rocks. *International Geology Review*, **60**: 1883-1905.
- Guan Q B, Liu Z H, Liu Y J, et al. 2019. Geochemistry and zircon U-Pb geochronology of mafic rocks in the Kaiyuan tectonic mélange of northern Liaoning Province, NE China: Constraints on the tectonic evolution of the Paleo-Asian Ocean. *Geological Journal*, **54**(2): 656-678.
- Hoskin P W O, Schaltegger U. 2003. The composition of zircon and igneous and metamorphic petrogenesis. *Reviews in Mineralogy and Geochemistry*, **53**: 27-62.
- Jackson S E, Pearson N J, Griffin W L, et al. 2004. The application of laser ablation-inductively coupled plasma-mass spectrometry to in situ U-Pb zircon geochronology. *Chemical Geology*, **211**(1): 47-69.
- Jahn B M, Wu F Y, Chen B. 2000. Granitoids of the Central Asian Orogenic Belt and continental growth in the Phanerozoic. *Transactions of The Royal Society of Edinburgh Earth Science*, **91**: 181-193.
- Jiang S H, Nie F J, Liu Y F, et al. 2010. Sulfur and lead isotopic compositions of Bairendaba and Weilasituo silver-polymetallic deposits, Inner Mongolia. *Mineral Deposits*, **28**: 101-112. (in Chinese with English abstract)
- Kelty T K, Yin A, Dash B, et al. 2008. Detrital-zircon geochronology of Paleozoic sedimentary rocks in the Hangay-Hentey basin, north-central Mongolia: Implications for the tectonic evolution of the Mongol-Okhotsk Ocean in central Asia. *Tectonophysics*, **451**: 97-122.
- Koschek G. 1993. Origin and significance of the SEM cathodoluminescence from zircon. *Journal of Microscopy*, **171**: 223-232.
- Lee J, Williams I, Ellis D. 1997. Pb, U and Th diffusion in nature zircon. *Nature*, **390**: 159-162.
- Li J L, Chen J L, Bai J K, et al. 2013a. Orogenic sedimentology series II-sedimentations in intra-arc of orogenic belts. *Northwestern Geology*, **46**(2): 1-11. (in Chinese with English abstract)
- Li Y F, Gao X Y, Bian X F, et al. 2013b. LA-ICP-MS zircon U-Pb dating and geochemical characteristics of the Mesozoic volcanic rocks from Longjiang basin in northern Da Hinggan Mountains and their geological implications. *Geological Bulletin of China*, **32**(8): 1195-1211. (in Chinese with English abstract)
- Li Y, Xu W L, Wang F, et al. 2017. Geochronology and geochemistry of late Paleozoic-early Mesozoic igneous rocks of the Erguna Massif, NE China: Implications for the early evolution of the Mongol-Okhotsk tectonic regime. *Asian Earth Sciences*, **144**: 205-224.
- Li J Y, Liu J F, Qu J F, et al. 2019. Paleozoic tectonic units of northeast China: Continental blocks or orogenic belts? *Earth Science*, **44**(10): 3157-3177. (in Chinese with English abstract)
- Li J, Tian Y, Cheng Y. 2023a. Late Jurassic Haobugao granites from the southern Great Xing'an Range, NE China: Implications for postcollision extension of the Mongol-Okhotsk Ocean. *Open Geosciences*, **15**(1): 20220567.
- Li X Y, Feng Z Q, Zhang Q H, et al. 2023b. Age of the "Precambrian" Fengshuigouhe Group in Lesser Xing'an Range and its tectonic implications: Evidence from zircon U-Pb dating and paleontological fossils. *World Geology*, **42**(2): 230-244. (in Chinese with English abstract)
- Li Y L, Zheng D, Li X B, et al. 2023c. New age constraints on the Lower Cretaceous Jiufengshan Formation of Inner Mongolia, China and their implications for the spatiotemporal development of the Jehol Biota. *Palaeogeography, Palaeoclimatology, Palaeoecology*, **629**: 111787.
- Liang C Y, Liu Y J, Zheng C Q, et al. 2019. Deformation patterns and timing of the thrust-nappe structures in the Mohe Formation in Mohe Basin, Northeast China: Implication of the closure timing of Mongol-Okhotsk Ocean. *Geological Journal*, **54**(2): 746-769.
- Liu J F, Chi X G, Dong C Y, et al. 2008a. Discovery of Early Paleozoic granites in the eastern Xiao Hinggan Mountains, northeastern China and their tectonic significance. *Geological Bulletin of China*, **27**(4): 534-544. (in Chinese with English abstract).
- Liu Z H, Wu X M, Zhu D F, et al. 2008b. Structural features

- and deformation stages of the Dayangshu Basin in northeast China. *Journal of Jilin University (Earth Science Edition)*, **38**(1): 27-33. (in Chinese with English abstract)
- Liu C F, Zhou Z G, Tang Y J, et al. 2017a. Geochronology and tectonic settings of Late Jurassic-Early Cretaceous intrusive rocks in the Ulanhot region, central and southern Da Xingan Range. *Geological Magazine*, **154**(5): 923-945.
- Liu Y J, Li W M, Feng Z Q, et al. 2017b. A review of the Paleozoic tectonics in the eastern part of Central Asian Orogenic Belt. *Gondwana Research*, **43**: 123-148.
- Liu Y J, Li W M, Ma Y F, et al. 2021. An orocline in the eastern Central Asian Orogenic Belt. *Earth-Science Reviews*, **221**: 103808.
- Liu H Y, McKenzie N R, Colleps C L, et al. 2022. Zircon isotope-trace element compositions track Paleozoic-Mesozoic slab dynamics and terrane accretion in Southeast Asia. *Earth and Planetary Science Letters*, **578**: 117298.
- Mi K F, Liu Z J, Li C F, et al. 2017. Origin of the Badaguan porphyry Cu-Mo deposit, Inner Mongolia, northeast China: Constraints from geology, isotope geochemistry and geochronology. *Ore Geology Reviews*, **81**: 154-172.
- Miao L C, Fan W M, Zhang F Q, et al. 2003. SHRIMP zircon geochronological study of the Xinkai-Ke Luo complex in the northwestern part of the Lesser Khingan Range and its implications. *Chinese Science Bulletin*, **48**(22): 2315-2323. (in Chinese with English abstract)
- Miao L C, Zhang F Q, Zhu M S, et al. 2015. Zircon SHRIMP U-Pb dating of metamorphic complexes in the conjunction of the Greater and Lesser Xing'an ranges, NE China: Timing of formation and metamorphism and tectonic implications. *Journal of Asian Earth Sciences*, **114**: 634-648.
- Moecher D P, Samson S D. 2006. Differential zircon fertility of source terranes and natural bias in the detrital zircon record: Implications for sedimentary provenance analysis. *Earth and Planetary Science Letters*, **247**: 252-266.
- Ouyang H, Mao J, Zhou Z, et al. 2015. Late Mesozoic metallogeny and intracontinental magmatism, southern Great Xing'an Range, northeastern China. *Gondwana Research*, **27**: 1153-1172.
- Pupin J P. 1980. Zircon and granite petrology. *Contributions to Mineralogy and Petrology*, **73**(3): 207-220.
- Sengör A M C, Seidlengör B A, Natal'in V S. 1993. Burtman. Evolution of the Altaiid tectonic collage and Palaeozoic crustal growth in Eurasia. *Nature*, **364**: 299-307.
- Sengör A M C, Natal'in B A, Sunal G, et al. 2018. The tectonics of the Altaiids: Crustal growth during the construction of the continental lithosphere of central Asia between 750 and 130 Ma ago. *Annual Review of Earth Planetary Sciences*, **46**(1): 439-494.
- She H Q, Li J W, Xiang A P, et al. 2012. U-Pb ages of the zircons from primary rocks in middle-northern Daxinganling and its implications to geotectonic evolution. *Acta Petrologica Sinica*, **28**(2): 571-594. (in Chinese with English abstract)
- Song Z W, Liang C Y, Neubauer F, et al. 2022. Multistage evolution of the Keluo complex in the northern Da Hinggan Mountains: Implications for the Mesozoic tectonic history of the eastern Central Asian Orogenic Belt. *Gondwana Research*, **107**: 339-369.
- Stewart J H, Gehrels G E, Barth A P, et al. 2001. Detrital zircon provenance of Mesoproterozoic to Cambrian arenites in the western United States and northwestern Mexico. *Geological Society of America Bulletin*, **113**: 1343-1356.
- Surpless K D, Graham S A, Covault J A, et al. 2006. Does the Great Valley Group contain Jurassic strata? Reevaluation of the age and early evolution of a classic foreland basin. *Geology*, **34**: 21-24.
- Tang J, Xu W L, Wang F, et al. 2013. Geochronology and geochemistry of Neoproterozoic magmatism in the Erguna Massif, NE China: Petrogenesis and implications for the breakup of the Rodinia supercontinent. *Pre-cambrian Research*, **224**: 597-611.
- Tang J, Xu W L, Wang F, et al. 2015. Geochronology, geochemistry, and deformation history of Late Jurassic-Early Cretaceous intrusive rocks in the Erguna Massif, NE China: Constraints on the late Mesozoic tectonic evolution of the Mongol-Okhotsk Orogenic Belt. *Tectonophysics*, **658**: 91-110.
- Tong H, Li G F, Xiang S M, et al. 2008. Analysis of basin evolvement and the geodynamics of Mesozoic Dayangshu Basin. *Journal of Daqing Petroleum Institute*, **32**(3): 111-113, 140-141. (in Chinese with English abstract)
- Vermeesch P. 2004. How many grains are needed for a provenance study? *Earth and Planetary Science Letters*, **224**(3/4): 441-451.
- Wang Y, Yang X P, Na F C, et al. 2017. Discovery of the Late Cambrian intermediate-basic volcanic rocks in Tahe, northern Da Hinggan Mountain and its geological significance. *Journal of Jilin University (Earth Science Edition)*, **47**(1): 126-138. (in Chinese with English abstract)
- Wilde S A. 2015. Final amalgamation of the Central Asian Orogenic Belt in NE China: Paleo-Asian Ocean closure

- versus Paleo-Pacific plate subduction—a review of the evidence. *Tectonophysics*, **662**: 345-362.
- Wu F Y, Yang J H, Lo C H, et al. 2007. The Heilongjiang Group: A Jurassic accretionary complex in the Jiamusi Massif at the western Pacific margin of northern Chain. *Island Arc*, **16**(1): 156-172.
- Wu F Y, Sun D Y, Ge W C, et al. 2011. Geochronology of the Phanerozoic granitoids in northeastern China. *Journal of Asian Earth Sciences*, **41**(1): 1-30.
- Xiao W J, Windley B F, Hao J, et al. 2003. Accretion leading to collision and the Permian Solonker suture, Inner Mongolia, China: Termination of the central Asian orogenic belt. *Tectonics*, **22**(6): 1069.
- Xiao W J, Windley B F, Huang B C, et al. 2009. End-Permian to mid-Triassic termination of the accretionary processes of the southern Altaids: Implications for the geodynamic evolution, Phanerozoic continental growth, and metallogeny of Central Asia. *International Journal of Earth Sciences*, **98**(6): 1219-1220.
- Xiao W J, Windley B F, Sun S, et al. 2015. A tale of amalgamation of three Permo-Triassic collage systems in Central Asia: Oroclines, sutures, and terminal accretion. *Annual Review of Earth Planetary Sciences*, **43**: 477-507.
- Xu W L, Pei F P, Wang F, et al. 2013. Spatial-temporal relationships of Mesozoic volcanic rocks in NE China: Constraints on tectonic overprinting and transformations between multiple tectonic regimes. *Journal of Asian Earth Sciences*, **74**: 167-193.
- Yang C J, Wang Y C. 2010. Zircon U-Pb age and the geological significance for Yichun Mesozoic granites in Southeast Lesser Khingan Range. *Jilin Geology*, **29**(4): 1-5, 31. (in Chinese with English abstract)
- Yang Y J, Jiang B, Wang X Z, et al. 2020. Chronostratigraphic division of the Early Cretaceous Jiufengshan Formation in Heibaoshan-Handaqi basin, Heilongjiang Province. *Geology and Resources*, **29**(5): 403-410. (in Chinese with English abstract)
- Zhang J H, Gao S, Ge W C, et al. 2010. Geochronology of the Mesozoic volcanic rocks in the Great Xing'an Range, northeastern China: Implications for subduction-induced delamination. *Chemical Geology*, **276**(3/4): 144-165.
- Zhang C, Wu X W, Zhang Y J, et al. 2018. Geochemistry and zircon LA-ICP-MS U-Pb age of volcanic rocks in Longjiang Formation of Longjiang Basin. *Geology in China*, **45**(3): 456-468. (in Chinese with English abstract)
- Zhang Q, Liang C Y, Liu Y J, et al. 2019. Final closure time of the Paleo-Asian Ocean: Implication from the provenance transformation from the Yangjiagou Formation to Lujiatun Formation in the Jiutai area, NE China. *Acta Petrologica Sinica (English Edition)*, **93**(5): 1456-1476.
- Zhao Z, Chi X G, Pan S Y, et al. 2010. Zircon U-Pb LA-ICP-MS dating of Carboniferous volcanics and its geological significance in the northwestern Lesser Xing'an Range. *Acta Petrologica Sinica*, **26**(8): 2452-2464. (in Chinese with English abstract)
- Zhao Y D, Che J Y, Wu D T, et al. 2017. Early-Middle Jurassic TTG Granites in northwest of Lesser Xing'an Range: Its geochronology, geochemical characteristics and tectonic significance. *Journal of Jilin University (Earth Science Edition)*, **47**(4): 1119-1137. (in Chinese with English abstract)
- Zhou J B, Wilde S A, Zhang X Z, et al. 2009. The onset of Pacific margin accretion in NE China: Evidence from the Heilongjiang high-pressure metamorphic belt. *Tectonophysics*, **478**: 230-246.
- Zhou J B, Wilde S A. 2013. The crustal accretion history and tectonic evolution of the NE China segment of the Central Asian Orogenic Belt. *Gondwana Research*, **23**(4): 1365-1377.
- Zhou J B, Wang B, Wilde S A, et al. 2015. Geochemistry and U-Pb zircon dating of the Toudaoqiao blueschists in the Great Xing'an Range, northeast China, and tectonic implications. *Journal of Asian Earth Sciences*, **97**: 197-210.